European Journal of Medicinal Chemistry 47 (2012) 125–137

Contents lists available at SciVerse ScienceDirect

European Journal of Medicinal Chemistry

journal homepage: http://www.elsevier.com/locate/ejmech

Original article

# 3,5-Disubstituted-thiazolidine-2,4-dione analogs as anticancer agents: Design, synthesis and biological characterization

Kai Liu [a], Wei Rao [a], Hardik Parikh [a], Qianbin Li [a], Tai L. Guo [b], Steven Grant [c], Glen E. Kellogg [a], Shijun Zhang [a,*]

[a] Department of Medicinal Chemistry, Virginia Commonwealth University, Richmond, VA, USA
[b] Department of Pharmacology and Toxicology, Virginia Commonwealth University, Richmond, VA, USA
[c] Department of Internal Medicine and Massey Cancer Center, Virginia Commonwealth University, Richmond, VA, USA

ARTICLE INFO

*Article history:*
Received 16 June 2011
Received in revised form
12 October 2011
Accepted 14 October 2011
Available online 21 October 2011

*Keywords:*
Thiazolidine-2,4-dione
Anticancer
Signaling pathways
Apoptosis
Multitarget molecule

ABSTRACT

A series of 2,5-disubstituted-thiazolidine-2,4-dione analogs based on the newly identified lead **1**, a potential anticancer agent via the inhibition of the Raf/MEK/extracellular signal regulated kinase (ERK) and phosphatidylinositol 3-kinase (PI3K)/Akt signaling cascades, were synthesized and biologically characterized. A new lead structure, **15**, was identified to have improved anti-proliferative activities in U937 cells, to induce apoptosis in U937, M12 and DU145 cancer cells, and to arrest U937 cells at the S-phase. Furthermore, Western blot analysis demonstrated a correlation of the anti-proliferative activity and blockade of the Raf/MEK/ERK and PI3K/Akt signaling pathways. Collectively, these results strongly encourage further optimization of **15** as a new lead with multi-target properties to develop more potent compounds as anticancer agents.

© 2011 Elsevier Masson SAS. All rights reserved.

## 1. Introduction

Cancer has surpassed heart disease as the leading cause of death in the United States in people younger than 85 and it is expected that 1.53 million cases of cancer will be diagnosed in the United States in 2010, among which more than 570,000 are expected to die [1]. In addition to the human cost, more than $72 billion is spent annually on cancer treatment, exacerbating problems with the overextended U.S. health care economy. While many chemotherapeutic strategies for cancer treatment have been proposed, tested and in some cases implemented in the past few decades, these diseases remain tenacious and deadly. Therefore, there is a desperate need to develop treatments with novel mechanisms to combat this disease.

Survival signaling pathways under growth factor loops have been implicated in cancer development, progression, and metastasis, among which the Raf/MEK/extracellular signal regulated kinase (ERK) and phosphatidylinositol 3-kinase (PI3K)/Akt signaling cascades are the most commonly up-regulated in human cancers [2–8]. More importantly, these two signaling pathways have been shown to function cooperatively to promote transformed cancer cell survival. For example, crosstalk and a feedback regulation between the Raf/MEK/ERK and PI3K/Akt pathways have been demonstrated recently, indicating the potential of interruption of more than one signaling pathway to optimize cytotoxic effects and to reduce drug resistance [5,9–14]. To further support this, several studies have demonstrated the synergistic effects in triggering cancer cell death by concomitant interruption of these two pathways both *in vitro* and *in vivo* using a combination regimen [12–18]. Collectively, these results implicate that development of novel compounds that can co-target the Raf/MEK/ERK and PI3K/Akt signaling pathways may represent an innovative strategy to provide clinically beneficial pharmacotherapy for human cancer.

Thiazolidine-2,4-dione (TZD) and rhodanine analogs have been recognized as the privileged templates in drug design and discovery [19,20] and numerous compounds containing the TZD ring have been developed as potential anticancer agents, such as the PI3K inhibitor GSK1059615 and its analogs [21]. More interestingly, some TZD analogs such as the anti-diabetic drug troglitazone have been shown to exhibit anticancer activities through the inhibition of the Raf/MEK/ERK signaling pathway [22]. Rhodanine compounds have been referred to as Pan Assay INterference

* Corresponding author. Department of Medicinal Chemistry, School of Pharmacy, Virginia Commonwealth University, 800 E. Leigh Street, Suite 205, Richmond, VA 23298-0540, USA. Tel.: +1 804 6288266; fax: +1 804 8287625.
*E-mail address:* szhang2@vcu.edu (S. Zhang).

0223-5234/$ – see front matter © 2011 Elsevier Masson SAS. All rights reserved.
doi:10.1016/j.ejmech.2011.10.031

compounds (PAINs) by one group [23]. TZD compounds, differing by only one atom from rhodanine (S to O), can produce completely different pharmacological effects [24] and the success of TZD analogs in preclinical and clinical trials may well support the potential of such molecules as lead structures in developing anticancer agents. Recently, we identified a TZD analog **1** with potential anticancer activity mainly through the inhibition of the Raf/MEK/ERK and PI3K/Akt signaling pathways (Fig. 1) [25,26]. Herein, we report the structure–activity relationship (SAR) studies of **1** to shed light on the structural features that are critical to their biological activity. One new lead compound with improved potency was identified to inhibit the growth of multiple cancer cell lines via the inhibition of the Raf/MEK/ERK and PI3K/Akt signaling cascades, to induce apoptosis as well as to interfere with the cell cycle transition.

## 2. Molecular design and chemistry

In order to obtain information of structural features in **1** that are critical to the anticancer activity, compound **1** was divided into three domains for structural modification and optimization: 1) phenyl ring domain; 2) ethylamine domain; and 3) TZD domain. As shown in Fig. 1, compounds **2**–**10** were designed to evaluate how the electrostatic and steric nature of the substituents on the phenyl ring will influence the biological activity. Compounds **11**–**13** were designed to examine whether the bioisosteric replacement of benzene ring with pyridine or indole ring will be tolerated or improve activity. The design and characterization of compounds **14**–**16** will help shed light on the roles of the aromatic ring in biological activity. Compounds **17**–**19** were designed to evaluate whether the primary amine is critical or a functional group with similar H-bond interactions will retain the activity. Compounds **20** (racemic) and **21** were designed to investigate the role of the exocyclic double bond and the TZD ring.

The synthesis began with the preparation of various aldehydes as shown in Scheme 1. Briefly, substituted benzaldehydes (**22**), *N*-Boc-indole-3- or -5-carbaldehyde (**23** or **24**), or cyclopropanecarbaldehyde (**25**) were converted to their Meldrum's acid derivatives **26** followed by reduction and hydrosilylation to give various aldehydes **29** [27]. The synthesis of cyclohexyl-propionaldehyde and 3-pyridin-3-yl-propionaldehyde was achieved through the Swern oxidation of 3-cyclohexyl-propanol **27** and 3-pyridin-3-yl-propanol **28**, respectively. Then, Knoevenagel condensations [28] of aldehydes **29** with **31**, **32**, **33** or **34** that were synthesized from the alkylation reactions of TZD with (2-bromo-ethyl)-carbamic acid *tert*-butyl ester, 2-bromoethanol, 2-bromo-acetic acid *tert*-butyl ester, or 4-(2-bromo-ethyl)-morpholine followed by removal of Boc or *tert*-butyl ester group afforded compounds **2**–**8** and **11**–**19**. The synthesis of **20** was achieved through Pd–C catalyzed hydrogenation of lead **1**.

The synthesis of **9** and **10** was shown in Scheme 2. The reaction of 4-iodo-phenylamine **35** with methanesulfonyl chloride afforded **36**, which after Heck coupling reaction with allyl alcohol under the catalysis of palladium (II) acetate gave aldehyde **37**. Similarly, aldehyde **40** was synthesized from **38**. Then, Knoevenagel condensations of **37** and **40** with **31** followed by removal of Boc group yielded compounds **9** and **10**, respectively.

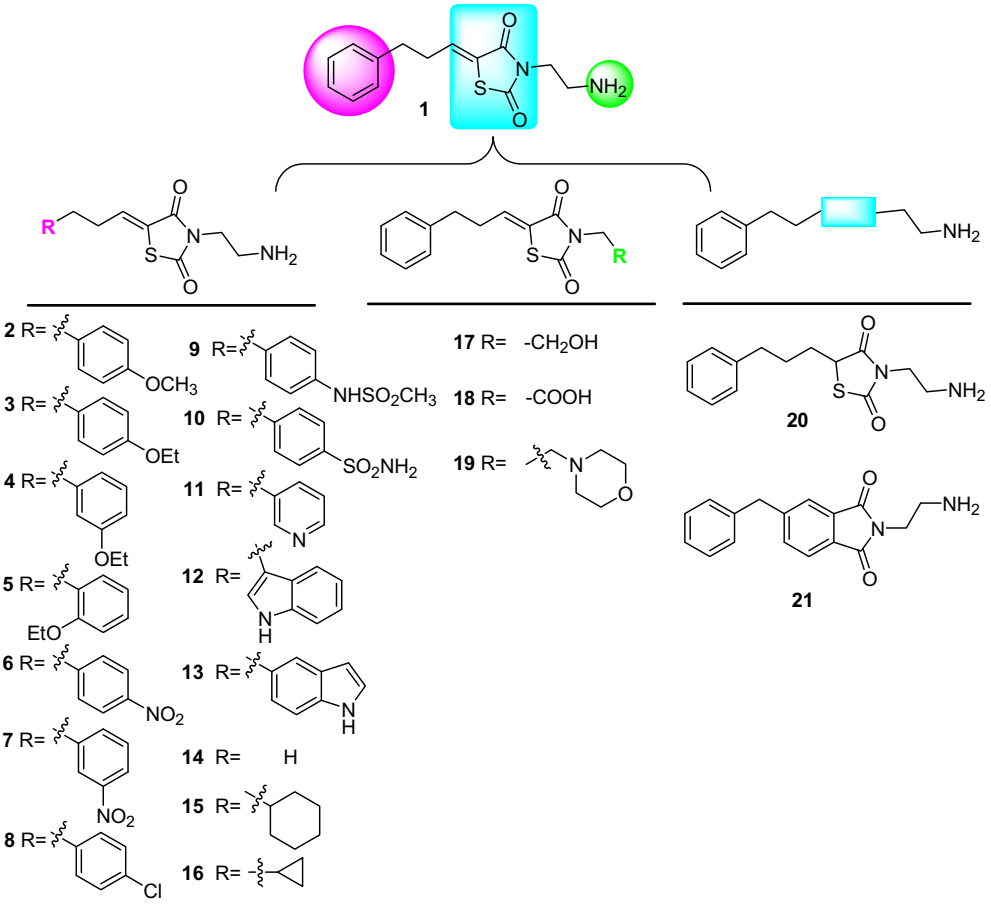


**Fig. 1.** Lead compound **1** and newly designed analogs.

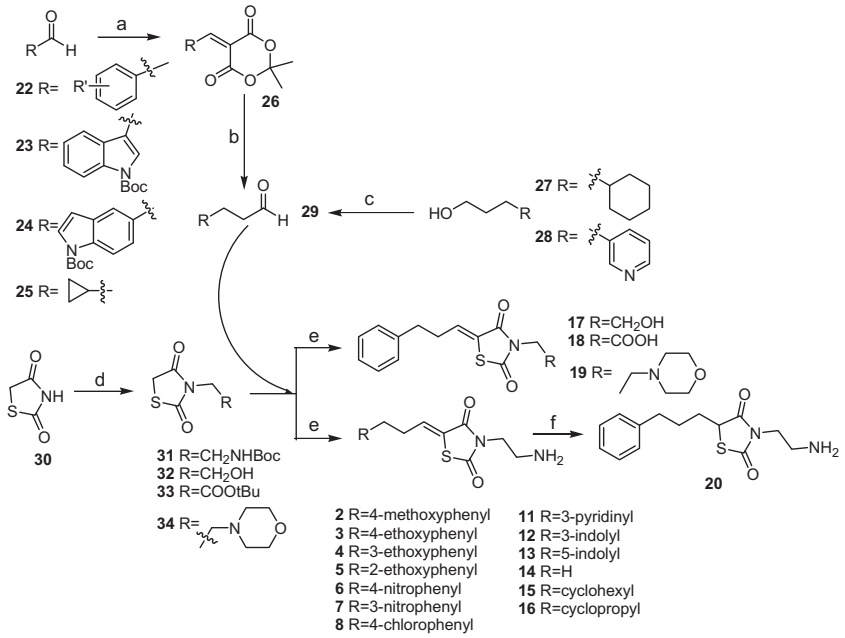

**Scheme 1.** Reagents and conditions: a) Meldrum's acid, piperidine, EtOH; b) i. $NaBH_4$, AcOH, $CH_2Cl_2$; ii. $PhSiH_3$, $Et_3N$, THF; c) DMSO, $(COCL_2)$, $Et_3N$, $CH_2Cl_2$; d) $BrCH_2CH_2NHBoc$, or $BrCH_2CH_2OH$, or 2-bromo-acetic acid *tert*-butyl ester, or 4-(2-bromo-ethyl)-morpholine, $K_2CO_3$, TZD, TBAI, acetone; e) i. piperidine EtOH, reflux, ii. 1,4-Dioxane–HCl or TFA/$CH_2Cl_2$; f) Pd/C, $H_2$, MeOH.

As shown in Scheme 3, coupling reaction of mono Boc-protected 1,2-diaminoethane with trimellitic anhydride **41** followed by reduction with $BH_3$ in THF afforded **43** in good yield. Esterification of **43** with diethyl chlorophosphate gave intermediate **44**, which after Suzuki–Miyaura cross-coupling reaction with benzeneboronic acid in the presence of palladium (II) acetate and $PPh_3$ followed by the removal of Boc group afforded **21** in high yield [29].

## 3. Results and discussion

### 3.1. Growth inhibition of human leukemia U937 cells

The activation of the Raf/MEK/ERK and PI3K/Akt signaling pathways has been shown to play multiple roles in the proliferation and apoptosis of hematopoietic cells including U937 cells [5]. Furthermore, U937 cell line has been shown to be a good model in characterizing our compounds in our previous work [25,26]. Therefore, compounds **1**–**21** were first tested for their inhibitory effects on the growth of U937 cells to identify active compounds. As shown in Table 1, no growth inhibition was observed for compounds **14** and **20** at concentrations up to 30 μM highlighting the essential role of the aromatic ring and the exocyclic double bond to the biological activity. **21** did not show inhibitory effects on the growth of U937 cells either, which further highlights the critical role of the exocyclic double bond in the activity of **1** as this double bond is incorporated into the benzene ring in **21**. Notably, **15** exhibited enhanced growth inhibition compared to **1** (~3 fold increase) in U937 cells. This may suggest an important role of steric effects at this specific domain as the phenyl ring in **1** is planar while the cyclohexane ring in **15** is non-planar with possible chair, boat, or other transitional conformations. This notion was further supported by the fact that **16** with a cyclopropane ring exhibited decreased growth inhibition activity in U937 cells. Compounds **2**–**5** with electron-donating substitutions on the phenyl ring of **1** exhibited comparable potency to **1**. On the other hand, compounds with electron-withdrawing substitutions on the phenyl ring exhibited decreased growth inhibition of U937 cells (**6**–**8**) compared to **1**. Interestingly, introduction of sulfonamide substitutions at the *para*-position of **1** led to a total loss of activity as demonstrated by **9** and **10**. This may indicate that protein interactions introduced by the sulfonamide moieties other than steric effects are not favored at this specific domain as **3** with an ethoxy group exhibited comparable potency to **1**. This is somewhat echoed by the decreased potency of compounds **11**–**15** with the bioisosteric replacement of phenyl ring with a pyridine or an indole ring, respectively.

Replacement of the $NH_2$ of the ethylamine with carboxyl (**18**) or tertiary amino (**19**) groups led to significant decrease or total loss of

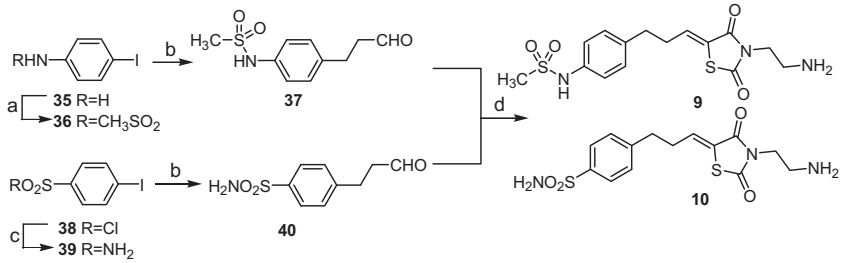

**Scheme 2.** Reagents and conditions: a) $CH_3SO_2Cl$, $Et_3N$, $CH_2Cl_2$; b) Allyl alcohol, $NaHCO_3$, TBACl, $Pd(OAc)_2$, DMF; c) $NH_4OH$; d) i. 13, piperidine EtOH, reflux; ii. 1,4-Dioxane–HCl.

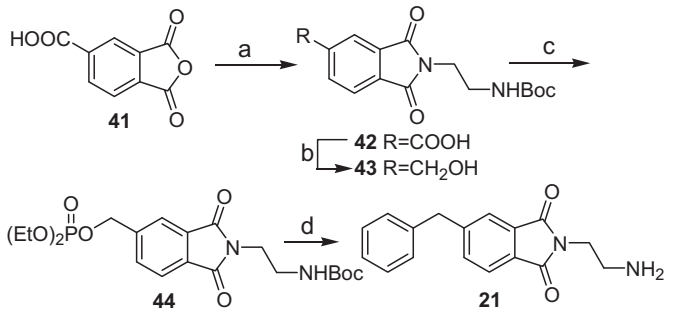


**Scheme 3.** Reagents and conditions: a) $NH_2CH_2CH_2NHBoc$ THF, $Et_3N$; b) $BH_3$, THF; c) diethyl chlorophosphate, $Et_3N$, THF, DMAP; d) i. Benzeneboronic acid, $Pd(OAc)_2$, $PPh_3$, $K_3PO_4$, toluene; ii. 1,4-Dioxane–HCl.

**Table 1**
Growth inhibition of U937 cells by **1**–**21** (μM).

| Compound | $IC_{50}$ ± SEM | Compound | $IC_{50}$ ± SEM |
|---|---|---|---|
| **1** | 10.4 ± 0.025 | **12** | 29.5 ± 0.12 |
| **2** | 9.4 ± 0.015 | **13** | 27.7 ± 0.11 |
| **3** | 9.6 ± 0.040 | **14** | >30 |
| **4** | 10.0 ± 0.13 | **15** | 3.4 ± 0.043 |
| **5** | 11.3 ± 0.17 | **16** | 14.1 ± 0.010 |
| **6** | >30 | **17** | 11.3 ± 0.031 |
| **7** | 24.4 ± 0.21 | **18** | >30 |
| **8** | 21.2 ± 0.089 | **19** | >30 |
| **9** | >30 | **20** | >30 |
| **10** | >30 | **21** | >30 |
| **11** | >30 | | |

activity, which highlights the important role of primary amine. Interestingly, replacement of the $NH_2$ with an OH (**17**) can maintain the biological activity in U937 cells. These results may suggest that H-bond interactions instead of ionic interactions with certain acidic amino acid residues in the target protein(s) are important for biological activity while steric effects are not favored at this specific site.

### *3.2. Effects of **15** on the Raf/MEK/ERK and PI3K/Akt signaling pathways*

To confirm whether the growth inhibition of U937 cells was mediated through the inhibition of the Raf/MEK/ERK and PI3K/Akt signaling cascades as seen in **1**, **15** was examined by Western blot analysis in U937 cells. As shown in Fig. 2A, **15** consistently suppressed the expression of the p-MEK, p-ERK and p-Akt levels, critical components of these two signaling pathways, at a concentration as low as 3 μM, indicating that signaling blockage and growth inhibition in U937 cells were correlated. This notion is further supported by the results of compounds **1** [26] and **20**, which showed decreased suppression or no suppression of the expression of these proteins compared to **15** (Fig. 2B and C), thus suggesting that **15** has potential as a new lead for developing more potent dual-pathway inhibitors. The level of p-4EBP1, a downstream substrate of these two signaling pathways, was also consistently suppressed. **15** did not inhibit other signaling pathways such as p38 and JNK signaling cascades (data not shown). To evaluate whether the anti-proliferative and signaling cascade inhibitory effects of **15** are cell specific, **15** was tested in androgen-insensitive prostate PC-3, DU145 and M12 cells. As shown in Fig. 3A, **15** exhibited growth inhibition on all three cancer cell lines comparable to the results from U937 cells. More importantly, **15** also consistently inhibited the PI3K/Akt and Raf/MEK/ERK signaling pathways as seen in the suppressed level of p-ERK and p-Akt in DU145 cells (Fig. 3B).

Next, to get preliminary target information, **15** was tested against a 52-kinase panel. As shown in Table 2, **15** significantly inhibited MEK1 and moderately inhibited PI3K consistent with the effects on p-MEK, p-ERK and p-Akt in our cell-based assays. The fact that the p-Raf level was not affected by treatment with **15** (Fig. 2A) may also support MEK as its potential target protein. Interestingly, **15** also inhibited 5′-adenosine monophosphate-activated protein kinase (AMPK). To confirm the inhibitory effects on AMPK, Western blot analysis was performed in U937 cells. Surprisingly, AMPK is activated upon treatment with **15** with an enhanced p-AMPK level (Fig. 2A). Discrepancies in results

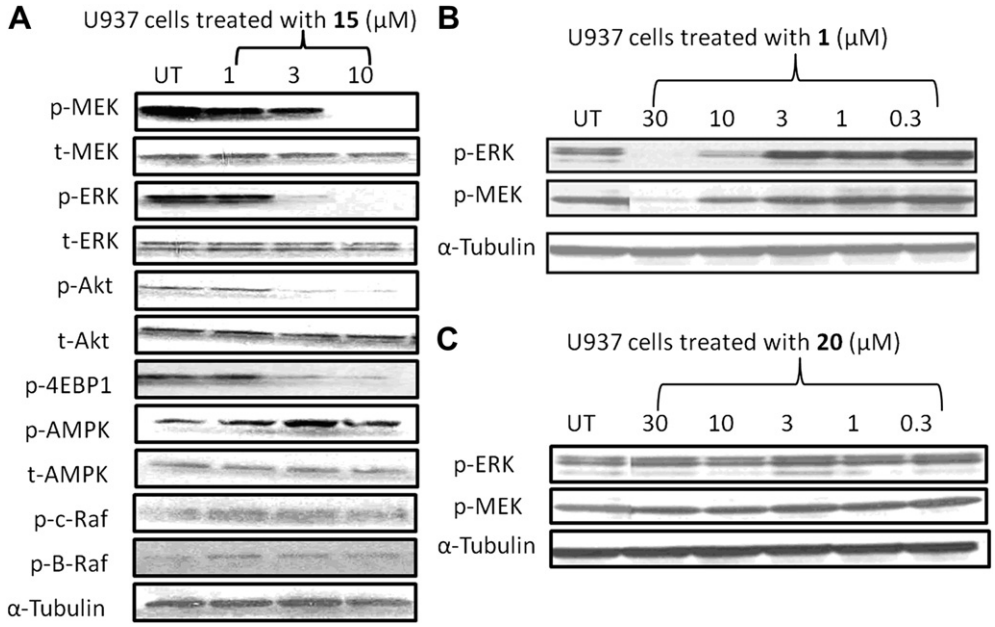


**Fig. 2.** U937 cells were treated with **15** (A), or **1** (B), or **20** (C) for 1 h, after which cell lysates were analyzed by Western blot using corresponding primary antibodies. The image of Western blot represents the results from one of three independent experiments.

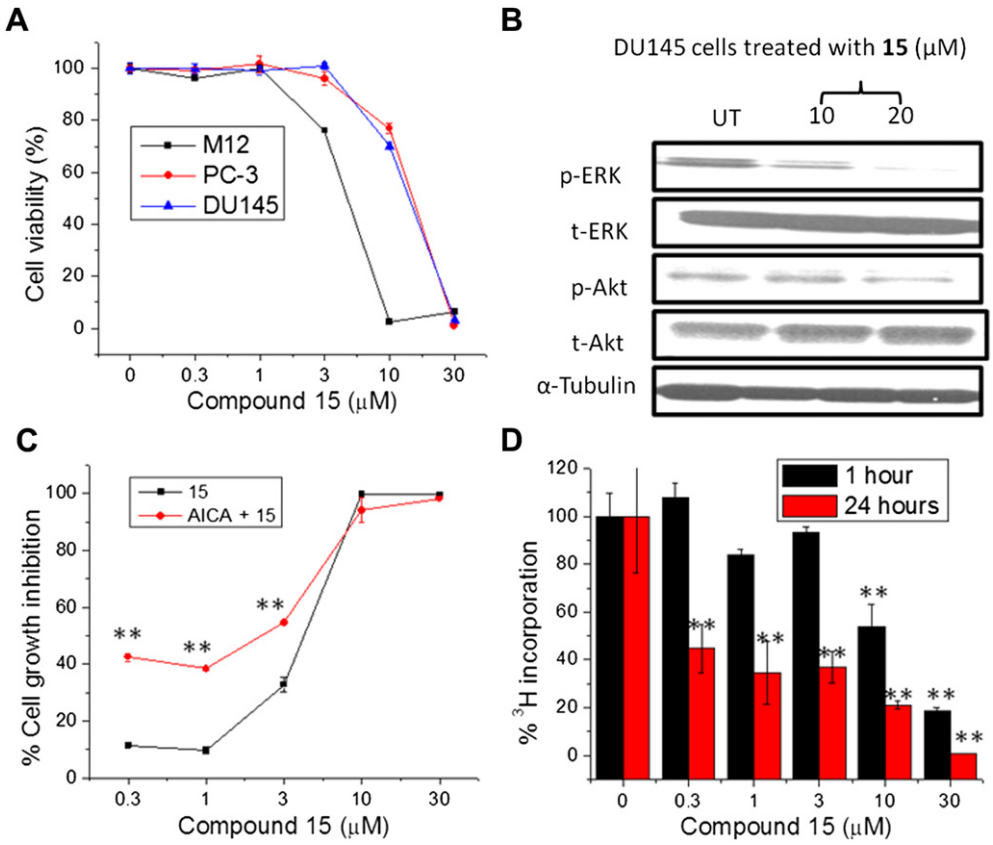


**Fig. 3.** A. M12, PC-3 and DU145 cells were treated with **15** for 24 h and the cell viability was analyzed by MTS; B. DU145 cells were treated with **15** at indicated concentrations for 24 h. Lysates from cultures were analyzed by Western blotting using corresponding primary antibodies; C. U937 cells were treated with **15** with or without the presence of AICA (320 μM) for 72 h, then growth inhibition was analyzed by MTS assay. Data were expressed as mean percentage viability ($n = 6$). Error bars represent standard error of mean (SEM); D. U937 cells were treated with **15** in the presence of 1 μCi [$^3$H]-thymidine. Cells were collected and the radioactivity was counted ($^3$H-thymidine incorporation is 3428 ± 338 and 183754 ± 43264 cpm/20,000 cells for 1 h and 24 h control, respectively). $^{**}P < 0.01$ indicates significant differences from control group analyzed by one-way ANOVA.

from isolated kinase assays compared to results obtained against whole cell assays may exist due to assay conditions; thus, we believe that assay results from human cancer cells may deliver the most meaningful information. To further confirm **15**'s activation of AMPK, the effects of AICA (5-amino-4-imidazole carboxamide) on the growth inhibition of U937 cells by **15** were tested. AICA is metabolized to AICAR (5-amino-4-imidazolecarboxamide ribonucleotide) and has been shown to activate AMPK [30–32]. Addition of AICA would be expected to mitigate the growth inhibition of U937 cells by **15** if **15** inhibits AMPK and this inhibition precipitates the lethal effects of **15** in U937 cells. As shown in Fig. 3C, the addition of AICA (320 μM) enhanced the growth inhibition of U937 cells by **15**. Since AICA does not produce cytotoxic effects by itself at the tested concentration (data not shown), clearly **15** activates AMPK, which is consistent with the Western blot results (Fig. 2A). It has been documented that activation of AMPK leads to the suppression of mTOR [33], the direct downstream substrate of Akt. Therefore, the activating effects of **15** on AMPK suggest additional benefits of our proposed approach in treating cancer. **15** also inhibited CaMK

**Table 2**
Selectivity of **15**.[a]

| Kinase | % Inhibition | Kinase | % Inhibition | Kinase | % Inhibition | Kinase | % Inhibition |
|---|---|---|---|---|---|---|---|
| ABL | 6 | c-TAK1 | 6 | LCK | 4 | PI3Ka | 45 |
| AKT1 | 3 | DYRK1a | −5 | LYN | 0 | PIM2 | 38 |
| AKT2 | 8 | Erk1 | 21 | MAPKAPK2 | 3 | PKA | −3 |
| AMPK | 76 | Erk2 | 11 | MARK1 | 0 | PKCb2 | 16 |
| AurA | −4 | FGFR1 | 3 | MEK1 | 69 | PKCz | −8 |
| BTK | 12 | FLT3 | 38 | MEK2 | 27 | PKD2 | 0 |
| CAMK2 | 60 | FYN | 0 | MET | −1 | PKGa | −2 |
| CAMK4 | 71 | GSK3b | 0 | MSK1 | 6 | PRAK | 4 |
| CDK2 | −2 | HGK | −1 | MST2 | 3 | ROCK2 | −1 |
| CHK1 | 11 | IGF1R | −5 | P38a | −13 | RSK1 | 2 |
| CHK2 | 8 | INSR | −2 | P70S6K | 5 | SGK1 | 14 |
| Ckld | −5 | IRAK4 | −1 | PAK2 | 10 | SRC | 2 |
| c-Raf | −1 | KDR | −28 | PDK1 | −2 | SYK | 9 |

[a] The effects of **15** on the indicated protein kinases were determined through the Rapid KinaseAdvisor profiling service from Caliper Life Sciences. Values represent the percent inhibition of each kinase at 10 μM of the test compound and are the average of two independent experiments ($n = 2$).

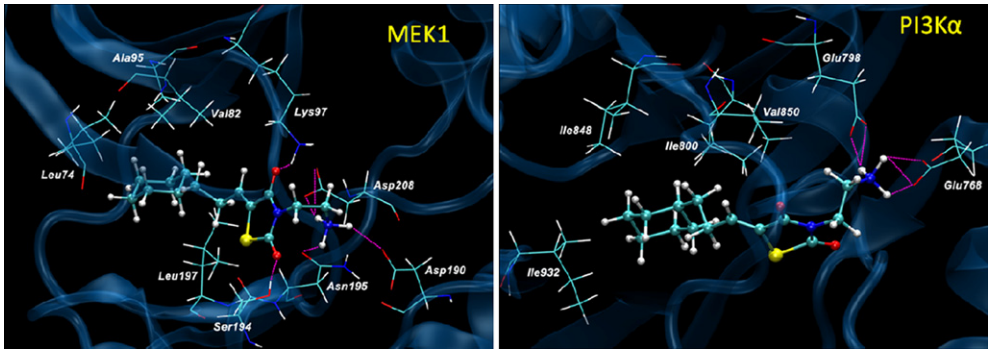


**Fig. 4.** Docking studies of **15** into MEK1 and PI3Kα.

($Ca^{2+}$/calmodulin-dependent protein kinases 2/4) in this screening test. Since CaMKs are involved in the upstream of both the Raf/MEK/ERK and PI3K/Akt signaling pathways, immunoblot assays of certain protein levels may not reflect the true interactions of **15** with CAMKs and further studies will be required to confirm the inhibitory effects of **15** on CaMKs. Taken together, the results suggest that **15** may function as a multi-target molecule that exhibits anti-proliferative activity mainly through the Raf/MEK/ERK and PI3K/Akt signaling pathways.

### 3.3. *Effects of **15** on the DNA synthesis of U937 cells*

In order to examine the effects on short-term DNA synthesis and to confirm the anti-proliferative activity, **15** was tested in U937 cells using [$^3$H]-thymidine incorporation assay. As shown in Fig. 3D, **15** significantly inhibited the DNA synthesis at as early as 1 h treatment at higher concentrations (10 and 30 μM). After 24 h treatment, **15** exhibited significant inhibition on DNA synthesis of U937 cells at all tested concentrations. However, **15** did not show cytotoxic effects at lower concentrations (0.3 and 1 μM) when tested using MTS assay. These results appear to indicate that **15** is able to inhibit the synthesis of DNA without significant lethal effects on U937 cells after a short-term treatment.

To further evaluate its effects on other human cancer cells, **15** was tested against the National Cancer Institute (NCI)'s 60 cancer cell lines (data not shown). As anticipated, **15** consistently inhibited the cancer cells at $GI_{50}$ values (50% of growth inhibition) ranging from 1.40 μM–5.10 μM, which indicates its potential as a lead compound for broad-spectrum anticancer agents.

### 3.4. *Molecular modeling studies*

Since **15** exhibits dual-inhibition of MEK1 and PI3K through the kinase screening, it would be of interest to get some information

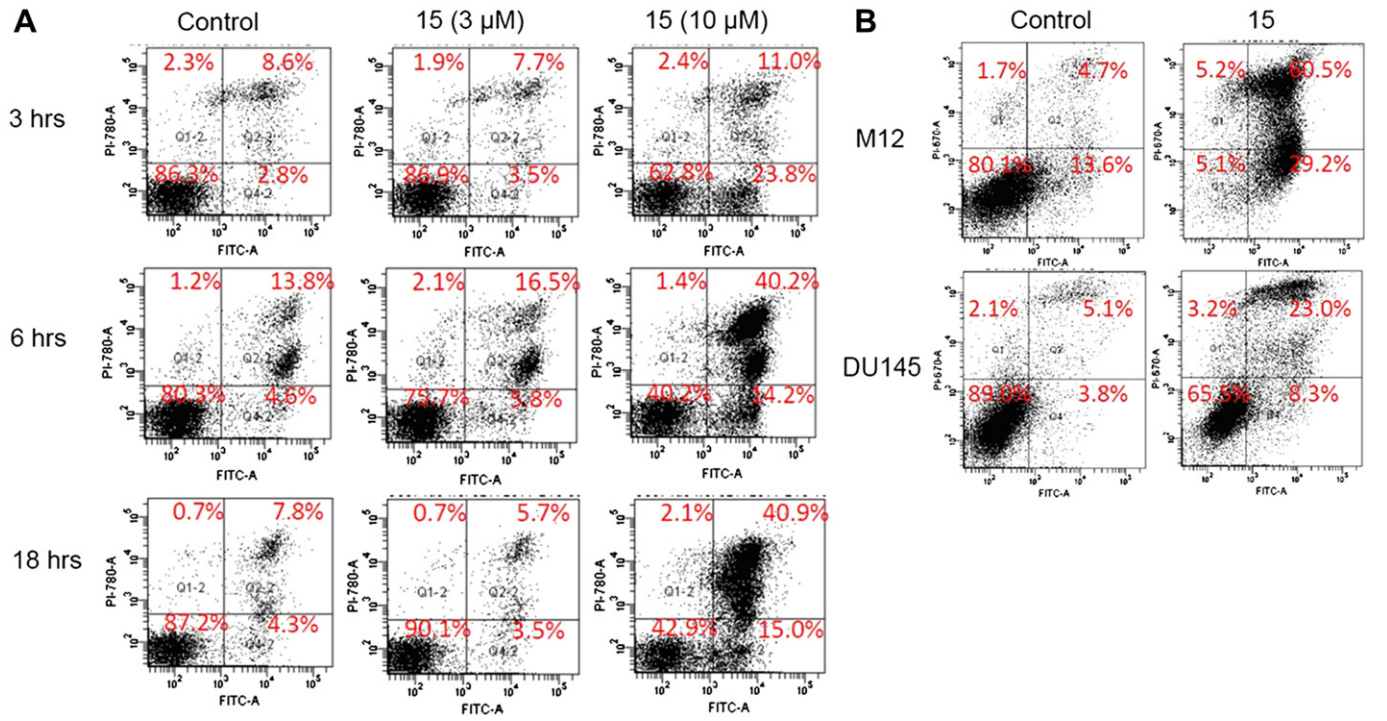


**Fig. 5.** **15** induces apoptosis in U937, M12 and DU145 cells. A. U937 cells were treated with **15** for indicated time, after which the cells were stained with Annexin V/PI and analyzed by flow cytometry; B. Indicated cancer cells were treated with **15** (20 μM) for 24 h. The cells were then stained with Annexin V/PI and analyzed by flow cytometry. The upper right represents late apoptosis as detected by annexin V/Pi staining; the lower right represents early apoptosis as detected by only annexin V staining; the total percentage from upper right and lower right was referred as the percentage of apoptosis. The image represents the results from one of two independent experiments.

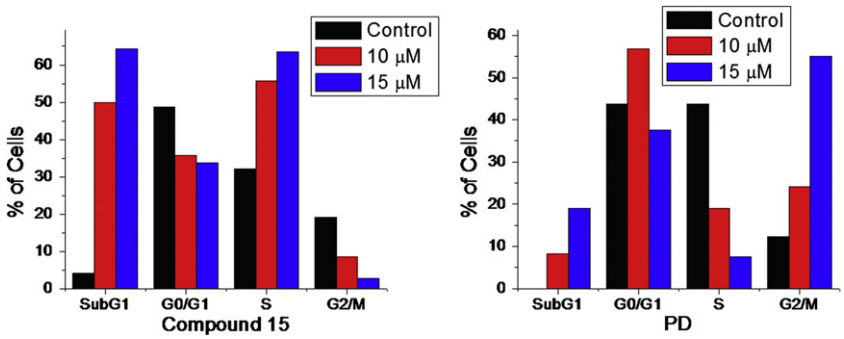


**Fig. 6.** Effects of **15** and PD184352 on the cell cycle of U937 cells. Cells were treated with **15** or PD184352 at indicted concentrations for 24 h and stained with PI. Then the cells were analyzed by flow cytometry.

about the nature of the interactions of this compound with these enzymes. Thus, **15** was initially docked into the ATP binding pockets of MEK1 and PI3K using GOLD 3.0 [34] as the binding sites of **15** on these two kinases are unknown. Briefly, the 3D structures of MEK1 (PDB ID 1s9j [35]) and PI3Kα (PDB ID 3hhm [36]) were modeled by adding hydrogens and minimizing using *Sybyl 7.2* (1000 iterations, Gasteiger-Hückel charges, gradient of 0.05 kcal $mol^{-1}$ $Å^{-1}$). **15** was docked into the ATP binding pockets (50 positions per ligand; no early termination; no constraints) and the docked positions were scored using HINT [37]. The best docked positions were selected for minimization (2500 iterations, gradient of 0.005 kcal/mol Å). The docking results suggest that **15** fits nicely into the ATP binding pocket of both MEK1 and PI3K. As shown in Fig. 4, **15** interacts with the MEK1 through H-bond interactions of the ethylamine with the Asp190, Asn195 and Asp208 residues. The two carbonyl groups of TZD also interact with Lys97 and Ser194 through H-bonds. The cyclohexane ring of **15** fits into a hydrophobic pocket that consists of Leu74, Val82, Ala95 and Leu197. Similarly, the ethylamine interacts with Glu768 and Glu798 of PI3K through H-bond interactions and the cyclohexane ring interacts with the residues of Ile800, Ile848 and Ile932 through hydrophobic interactions. When ERK2 (PDB ID 3erk) was examined as a control, no favorable interactions were observed for **15** in the ATP binding pocket (data not shown). Taken together, the preliminary docking studies also support the results of **15** concluded from the anti-proliferation studies in U937 cells.

### 3.5. *Effects of **15** on the apoptosis and cell cycle of U937 cells*

The Raf/MEK/ERK and PI3K/Akt signaling cascades play important roles in the regulation of apoptosis and the $G_1$-S and $G_2$-M transition in the cell cycle [5,38,39]. To get preliminary mechanistic information for **15**'s anti-proliferative activity, the apoptotic effects of **15** on U937, M12 and DU145 cells were evaluated. As shown in Fig. 5A, **15** induced apoptosis at as early as 3 h in U937 cells (23.4% increase) and longer exposure to **15** (18 h) significantly induced apoptosis in U937 cells (43.8% increase) at 10 μM concentration. **15** (20 μM) significantly induced apoptosis in M12 (71.4% increase) while moderately induced apoptosis in DU145 cells (22.5% increase) after 24 h treatment (Fig. 5B). Furthermore, we have confirmed that reactive oxygen species (ROS) are not involved in the lethal effects of **15** on these cancer cells (data not shown).

When the cell cycle of U937 cells was evaluated (Fig. 6), **15** dose-dependently arrested U937 cells at the S-phase (23.6% and 31.4% increase at 10 and 15 μM, respectively), an event accompanied with decrease of the $G_1/G_0$ and $G_2/M$ populations. The apoptotic effects as measured by the sub-diploid apoptotic fraction (49.9% and 64.3% at 10 and 15 μM respectively) were also consistent with the results from apoptosis assay (Fig. 5A). On the other hand, treatment of U937 cells with the MEK inhibitor PD184352 [40] arrested U937 cells at the $G_2/M$ phase, an event accompanied with significant decrease of the S-phase population. The different effects exhibited by PD184352 and **15** in cell cycle may be due to their having different inhibitory effects on the PI3K/Akt signaling pathway. Further studies such as evaluation of the levels of cyclins, p21 and p27 are warranted to better understand the mechanistic information of **15** on cell cycle progress.

## 4. Conclusion

In summary, a series of TZD analogs of **1** were designed and synthesized. Biological characterization of these analogs in human leukemia U937 cells established that steric interaction at the aromatic domain, the exocyclic double bond, and the H-bond interaction at the ethylamine domain are critical to the growth inhibition of cancer cells. One new lead compound, **15**, was identified to have improved anti-proliferative activity in U937 cells. More importantly, a close correlation was confirmed between the anti-proliferative activity and blockade of the Raf/MEK/ERK and PI3K/Akt signaling pathways. Compound **15** may execute its anti-proliferative activity through apoptotic effects in U937, M12 and DU145 cancer cells. Furthermore, **15** arrested U937 cells at the S-phase. In addition, it was discovered that **15** inhibits both MEK and PI3K, the critical kinases involved in the signal transduction of the Raf/MEK/ERK and PI3K/Akt cascades. Collectively, these results strongly suggest the potential of **15** as a new lead compound with multi-target properties and encourage further optimization of **15** to develop more potent and effective analogs as anticancer agents.

## 5. Experimental

### 5.1. *Chemistry*

Reagents and solvents were obtained from commercial suppliers and used as received unless otherwise indicated. All reactions were carried out under inert atmosphere ($N_2$) unless otherwise noted. Reactions were monitored by thin-layer chromatography (TLC) (pre-coated silica gel 60 $F_{254}$ plates, EMD Chemicals) and visualized with UV light or by treatment with phosphomolybdic acid. Flash chromatography was performed on silica gel (200–300 mesh, Fisher Scientific) using solvents as indicated. $^1H$ NMR and $^{13}C$ NMR spectra were routinely recorded on Bruker ARX 400 spectrometer. The NMR solvent used was $CDCl_3$ or DMSO-$d_6$ as indicated. Tetramethylsilane (TMS) was used as

internal standard. The purity of target compounds was determined by elemental analysis (Atlantic Microlab, Inc.).

### 5.2. Procedure A. Preparation of various intermediates **26** through Meldrum's acid

To a stirred solution of various substituted benzaldehydes or *N*-Boc-indole-carbaldehydes or cyclopropanecarbaldehyde (10.0 mmol) and Meldrum's acid (10.0 mmol) in EtOH (20.0 mL) was added piperidine (one drop), then the resulting solution was heated to reflux for 5 h and cooled to room temperature. The reaction mixture was filtered to give a light yellow solid which was purified by flash chromatography (hexane/acetone = 5/1) to give intermediate **26**.

#### 5.2.1. 5-(3-Cyclopropyl-methylene)-2,2-dimethyl-1,3-dioxane-4,6-dione

$^1$H NMR (400 MHz, $CDCl_3$): $\delta$ 7.21–7.18 (d, $J$ = 11.9 Hz, 1H), 3.25–3.20 (m, 1H), 1.75 (s, 6H), 1.47–1.45 (m, 2H), 1.11–1.09 (m, 2H).

#### 5.2.2. 5-(3-(4-Methoxyphenyl)-methylene)-2,2-dimethyl-1,3-dioxane-4,6-dione

$^1$H NMR (300 MHz, $CDCl_3$): $\delta$ 8.38 (s, 1H), 8.24–8.21 (d, $J$ = 9.3 Hz, 2H), 6.99–6.97 (d, $J$ = 9.3 Hz, 2H), 3.91 (s, 3H), 1.79 (s, 6H).

#### 5.2.3. 5-(3-(4-Ethoxyphenyl)-methylene)-2,2-dimethyl-1,3-dioxane-4,6-dione

$^1$H NMR (300 MHz, $CDCl_3$): $\delta$ 8.37 (s, 1H), 8.23 (d, $J$ = 9.3 Hz, 2H), 6.97 (d, $J$ = 9.3 Hz, 2H), 4.15 (q, $J$ = 7.0 Hz, 2H), 1.78 (s, 6H), 1.47 (t, $J$ = 6.9 Hz, 3H).

#### 5.2.4. 5-(3-(3-Ethoxyphenyl)-methylene)-2,2-dimethyl-1,3-dioxane-4,6-dione

$^1$H NMR (400 MHz, $CDCl_3$): $\delta$ 8.39 (s, 1H), 7.80 (s, 1H), 7.52–7.51 (d, $J$ = 7.7 Hz, 1H), 7.38 (t, $J$ = 8.1 Hz, 1H), 7.12–7.10 (d, $J$ = 8.2 Hz, 1H), 4.12–4.07 (q, $J$ = 7.0 Hz, 2H), 1.81 (s, 6H), 1.44 (t, $J$ = 7.0 Hz, 3H).

#### 5.2.5. 5-(3-(2-Ethoxyphenyl)-methylene)-2,2-dimethyl-1,3-dioxane-4,6-dione

$^1$H NMR (400 MHz, $CDCl_3$): $\delta$ 8.76 (s, 1H), 7.94–7.91 (d, $J$ = 7.8 Hz, 1H), 7.48 (t, $J$ = 7.9 Hz, 1H), 6.99 (t, $J$ = 7.4 Hz, 1H), 6.94–6.92 (d, $J$ = 8.4 Hz, 1H), 4.17–4.11 (q, $J$ = 7.0 Hz, 2H), 1.82 (s, 6H), 1.46 (t, $J$ = 7.0 Hz, 3H).

#### 5.2.6. 5-(3-(4-Nitrophenyl)-methylene)-2,2-dimethyl-1,3-dioxane-4,6-dione

$^1$H NMR (300 MHz, $CDCl_3$): $\delta$ 8.46 (s, 1H), 8.32–8.29 (d, $J$ = 9.3 Hz, 2H), 8.08–8.05 (d, $J$ = 9.3 Hz, 2H), 1.84 (s, 6H).

#### 5.2.7. 5-(3-(3-Nitrophenyl)-methylene)-2,2-dimethyl-1,3-dioxane-4,6-dione

$^1$H NMR (400 MHz, $CDCl_3$): $\delta$ 8.83 (t, $J$ = 1.8 Hz, 1H), 8.46 (s, 1H), 8.40–8.37 (d, $J$ = 8.2 Hz, 1H), 8.28–8.26 (d, $J$ = 7.9 Hz, 1H), 7.68 (t, $J$ = 8.0 Hz, 1H), 1.84 (s, 6H).

#### 5.2.8. 5-(3-(4-Chlorophenyl)-methylene)-2,2-dimethyl-1,3-dioxane-4,6-dione

$^1$H NMR (400 MHz, $CDCl_3$): $\delta$ 8.37 (s, 1H), 8.04–8.02 (d, $J$ = 8.7 Hz, 2H), 7.47–7.45 (d, $J$ = 8.7 Hz, 2H), 1.81 (s, 6H).

#### 5.2.9. 5-(N-Boc-indole-3-methylene)-2,2-dimethyl-1,3-dioxane-4,6-dione

$^1$H NMR (400 MHz, $CDCl_3$): $\delta$ 9.67 (s, 1H), 8.55 (s, 1H), 8.82 (s, 1H), 8.27–8.25 (d, $J$ = 8.0 Hz, 1H), 7.89–7.86 (d, $J$ = 8.0 Hz, 1H), 745–7.42 (m, 1H), 1.79 (s, 6H), 1.72 (s, 9H).

#### 5.2.10. 5-(N-Boc-indole-5-methylene)-2,2-dimethyl-1,3-dioxane-4,6-dione

$^1$H NMR (300 MHz, $CDCl_3$): $\delta$ 8.56 (s, 1H), 8.55 (s, 1H), 8.22–8.19 (d, $J$ = 9.0 Hz, 1H), 8.04–8.00 (dd, $J$ = 9.0 Hz, 1.8 Hz, 1H), 7.67–7.66 (d, $J$ = 3.9 Hz, 1H), 6.68–6.67 (d, $J$ = 3.9 Hz, 1H), 1.82 (s, 6H), 1.69 (s, 9H).

### 5.3. Procedure B. Preparation of various aldehydes **29** through Meldrum's acid derivative **26**

To a solution of various intermediates **26** (1.0 mmol) and acetic acid (1.5 mL) in dichloromethane (DCM) (9 mL) at 0 °C was added $NaBH_4$ (4.2 mmol) portion wise and the resulting solution was stirred at room temperature for 1 h. The reaction was then diluted with DCM (30.0 mL) and washed with brine and water. The organic layer was dried over anhydrous $Na_2SO_4$ and concentrated under vacuum. The residue was purified by flash chromatography (Hexane/acetone = 5/2) to give a light yellow oil which was treated with $Et_3N$ (2.0 mmol) followed by phenylsilane (3.0 mmol) in THF (10.0 mL). The resulting solution was stirred for 2 h at room temperature and quenched with $H_2O$. The reaction mixture was diluted with ethyl ether (30.0 mL) and washed with brine and water. The organic layer was dried over anhydrous $Na_2SO_4$ and concentrated under reduced pressure. The residue was purified by flash chromatography (Hexane/acetone = 5/1) to give **29** as light yellow oil. Most of the aldehydes synthesized through this procedure were directly added to the Knoevenagel condensation reactions as described in Procedure E without further purification and characterization.

#### 5.3.1. 3-Cyclopropyl-propionaldehyde

$^1$H NMR (400 MHz, $CDCl_3$): $\delta$ 9.80 (t, $J$ = 1.8 Hz, 1H), 2.55–2.51 (m, 2H), 1.57–1.51 (m, 2H), 0.71–0.67 (m, 1H), 0.48–0.43 (m, 2H), 0.07–0.04 (m, 2H).

#### 5.3.2. N-Boc-indole-3-yl-propionaldehyde

$^1$H NMR (400 MHz, $CDCl_3$): $\delta$ 9.87 (s, 1H), 8.13–8.11 (d, $J$ = 7.6 Hz, 1H), 7.52–7.50 (d, $J$ = 7.6 Hz, 1H), 7.37 (s, 1H), 7.34–7.30 (m, 1H), 7.27–7.23 (m, 1H), 3.04 (t, $J$ = 7.5 Hz, 2H), 2.86 (t, $J$ = 7.5 Hz, 2H), 1.66 (s, 9H).

### 5.4. Procedure C. Preparation of aldehydes **29** through Swern oxidation reaction

DMSO (14.0 mmol) was added dropwise to a stirred solution of oxalyl chloride (5.0 mmol) in DCM (20.0 mL) at −78 °C and the resulting reaction mixture was stirred for 20 min at this temperature. Then 3-cyclohexyl-propanol or 3-pyridinepropanol (4.0 mmol) was added dropwise and stirred for 1 h followed by the addition of $Et_3N$ (1.0 mL). The reaction was gradually brought to room temperature and $H_2O$ was added. The separated DCM phase was washed with brine and purified by flash chromatography (Hexane/ethyl acetate (EtOAc) = 10/1) to give a colorless oil.

#### 5.4.1. 3-Cyclohexyl-propionaldehyde

$^1$H NMR (400 MHz, $CDCl_3$): $\delta$ 9.77–9.76 (t, $J$ = 1.9 Hz 1H), 2.45–2.41 (dt, $J$ = 7.5, 1.9 Hz, 2H), 1.71–1.55 (m, 5H), 1.51–1.49 (m, 2H), 1.26–1.11 (m, 4H), 0.93–0.86 (m, 2H). $^{13}$C NMR (100 MHz, $CDCl_3$): 203.1, 41.5, 37.2, 33.0, 29.3, 26.4, 26.2.

### 5.5. Procedure D. Preparation of 3-substituted thiazoldine-2,4-diones **31**–**34**

A mixture of thiazolidine-2,4-dione (68.0 mmol), various bromide compounds (80.0 mmol), $K_2CO_3$ (92.0 mmol), TBAI

(6.8 mmol) in acetone (100.0 mL) was stirred at 40 °C for 10 h. The reaction mixture was cooled to room temperature and filtered through a short bed of celite and the filtrate was concentrated under vacuum. The residue was purified by flash chromatography (Hexane/EtOAc = 4/1 to 2/1) to give a white solid.

*5.5.1. tert-Butyl 2-(2,4-dioxo-thiazolidin-3-yl)-ethylcarbamate* ***31***

$^1$H NMR (300 MHz, $CDCl_3$): $\delta$ 3.94 (s, 2H), 3.78–3.74 (t, $J$ = 6.0 Hz, 2H), 3.40–3.34 (t, $J$ = 6.0 Hz, 2H), 1.43(s, 9H).

*5.5.2. 3-(2-Hydroxy-ethyl)thiazolidine-2,4-dione* ***32***

$^1$H NMR (400 MHz, $CDCl_3$): $\delta$ 3.99 (s, 2H), 3.86–3.81 (m, 4H).

*5.5.3. (2,4-Dioxo-thiazolidin-3-yl)-acetic acid tert-butyl ester* ***33***

$^1$H NMR (300 MHz, $CDCl_3$): $\delta$ 4.25 (s, 2H), 4.02 (s, 2H), 1.46 (s, 9H).

*5.5.4. 3-(2-Morpholino-ethyl)thiazolidine-2,4-dione* ***34***

$^1$H NMR (400 MHz, $CDCl_3$): $\delta$ 3.95 (s, 2H), 3.77–3.74 (t, $J$ = 6.4 Hz, 2H), 3.66–3.63 (t, $J$ = 4.6 Hz, 4H), 2.57–2.54 (t, $J$ = 6.4 Hz, 2H), 2.49–2.47 (t, $J$ = 4.6 Hz, 4H).

*5.6. Procedure E. Knoevenagel condensations of aldehydes* ***29*** *with* ***31–34*** *followed by the removal of Boc or tert-butyl ester group*

A solution of aldehyde **29** or propionaldehyde (0.5 mmol), 3-substituted-thiazolidine-2,4-dione (0.5 mmol) and piperidine (1 drop) in MeOH (3.0 mL) was stirred at room temperature overnight. The solvent was removed under reduced pressure and the residue was purified by flash chromatography (Hexane/acetone = 10/1). Products with Boc or *tert*-butyl ester group were treated with HCl (4.0 M in 1,4-dioxane) in EtOAc or trifluoroacetic acid in DCM to remove the protecting groups.

*5.6.1. 3-(2-Aminoethyl)-5-(3-(4-methoxyphenyl)propylidene) thiazolidine-2,4-dione* ***2***

$^1$H NMR (400 MHz, DMSO-$d_6$): $\delta$ 8.04 (brs, 3H), 7.11–7.08 (d, $J$ = 8.6 Hz, 2H), 6.96–6.92 (t, $J$ = 7.4 Hz, 1H), 6.80–6.78 (d, $J$ = 8.6 Hz, 2H), 3.78–3.75 (t, $J$ = 6.0 Hz, 2H), 3.67(s, 3H), 2.95–2.92 (t, $J$ = 6.0 Hz, 2H), 2.72–2.69 (t, $J$ = 7.4 Hz, 2H), 2.47–2.41 (m, 2H). $^{13}$C NMR (100 MHz, DMSO-$d_6$): 167.6, 164.5, 157.7, 137.4, 132.1, 129.2, 125.2, 113.8, 54.9, 36.6, 32.9, 32.1. Anal. ($C_{15}H_{19}ClN_2O_3S\cdot0.25H_2O$) Calcd. C: 51.87%, H: 5.66%, N: 8.06%; found C: 51.57%, H: 5.53%, N: 8.34%.

*5.6.2. 3-(2-Aminoethyl)-5-(3-(4-ethoxyphenyl)propylidene) thiazolidine-2,4-dione* ***3***

$^1$H NMR (400 MHz, DMSO-$d_6$): $\delta$ 8.05 (brs, 3H), 7.09–7.07 (d, $J$ = 8.6 Hz, 2H), 6.94 (t, $J$ = 7.4 Hz, 1H), 6.79–6.76 (d, $J$ = 8.6 Hz, 2H), 3.94–3.89 (q, $J$ = 7.0 Hz, 2H), 3.76 (t, $J$ = 6.0 Hz, 2H), 2.93 (m, 2H), 2.70 (t, $J$ = 7.4 Hz, 2H), 2.47–2.41 (m, 2H), 1.23 (t, $J$ = 7.0 Hz, 3H). $^{13}$C NMR (100 MHz, DMSO-$d_6$): 167.6, 164.5, 157.0, 137.4, 132.0, 129.3, 125.2, 114.3, 62.9, 36.6, 33.0, 32.1, 14.6. Anal. ($C_{16}H_{21}ClN_2O_3S$) Calcd. C: 53.85%, H: 5.93%, N: 7.85%; found C: 53.96%, H: 6.06%, N: 7.68%.

*5.6.3. 3-(2-Aminoethyl)-5-(3-(3-ethoxyphenyl)propylidene) thiazolidine-2,4-dione* ***4***

$^1$H NMR (400 MHz, DMSO-$d_6$): $\delta$ 8.06 (brs, 3H), 7.22–7.18 (t, $J$ = 7.9 Hz, 1H), 7.04–7.01 (t, $J$ = 7.4 Hz, 1H), 6.81 (s, 1H), 6.78–6.75 (m, 2H), 4.03–3.98 (q, $J$ = 7.0 Hz, 2H), 3.85–3.82 (t, $J$ = 6.0 Hz, 2H), 3.02–2.99 (t, $J$ = 6.0 Hz, 2H), 2.82–2.79 (t, $J$ = 7.4 Hz, 2H), 2.58–2.52 (m, 2H), 1.33–1.30 (t, $J$ = 7.0 Hz, 3H). $^{13}$C NMR (100 MHz, DMSO-$d_6$): 167.6, 164.5, 158.6, 141.8, 137.3, 129.4, 125.2, 120.4, 114.5, 112.1, 62.8, 36.6, 32.9, 32.5, 14.6. Anal. ($C_{16}H_{21}ClN_2O_3S\cdot0.25H_2O$) Calcd. C: 53.18%, H: 6.00%, N: 7.75%; found C: 53.11%, H: 5.98%, N: 7.88%.

*5.6.4. 3-(2-Aminoethyl)-5-(3-(2-ethoxyphenyl)propylidene) thiazolidine-2,4-dione* ***5***

$^1$H NMR (400 MHz, DMSO-$d_6$): $\delta$ 8.05 (brs, 3H), 7.21–7.16 (m, 2H), 7.08–7.05 (t, $J$ = 7.6 Hz, 1H), 6.96–6.94 (d, $J$ = 7.7 Hz, 1H), 6.89–6.85 (dt, $J$ = 1.0, 7.4 Hz, 1H), 4.08–4.02 (q, $J$ = 7.0 Hz, 2H), 3.85–3.82 (t, $J$ = 6.0 Hz, 2H), 3.01 (m, 2H), 2.81–2.78 (t, $J$ = 7.4 Hz, 2H), 2.52–2.50 (m, 2H), 1.40–1.36 (t, $J$ = 7.0 Hz, 3H). $^{13}$C NMR (100 MHz, DMSO-$d_6$): 167.6, 164.5, 156.4, 137.7, 129.8, 128.1, 127.8, 125.1, 120.2, 111.5, 63.1, 36.6, 31.4, 28.2, 14.7. Anal. ($C_{16}H_{21}ClN_2O_3S\cdot0.25H_2O$) Calcd. C: 53.18%, H: 6.00%, N: 7.75%; found C: 53.23%, H: 6.08%, N: 7.75%.

*5.6.5. 3-(2-Aminoethyl)-5-(3-(4-nitrophenyl)propylidene) thiazolidine-2,4-dione* ***6***

$^1$H NMR (400 MHz, DMSO-$d_6$): $\delta$ 8.19–8.17 (d, $J$ = 8.7 Hz, 2H), 7.88 (brs, 3H), 7.58–7.56 (d, $J$ = 8.7 Hz, 2H), 7.06–7.03 (t, $J$ = 7.5 Hz, 1H), 3.83–3.80 (t, $J$ = 5.8 Hz, 2H), 3.04–2.99 (m, 4H), 2.65–2.59 (m, 2H). $^{13}$C NMR (100 MHz, DMSO-$d_6$): 167.5, 164.5, 148.7, 146.1, 136.7, 129.7, 125.6, 123.5, 36.8, 32.7, 32.0. Anal. ($C_{16}H_{16}F_3N_3O_6S$) Calcd. C: 44.14%, H: 3.70%, N: 9.65%; found C: 43.93%, H: 3.78%, N: 9.70%.

*5.6.6. 3-(2-Aminoethyl)-5-(3-(3-nitrophenyl)propylidene) thiazolidine-2,4-dione* ***7***

$^1$H NMR (400 MHz, DMSO-$d_6$): $\delta$ 8.18 (s, 1H), 8.11–8.08 (d, $J$ = 7.8 Hz, 1H), 7.87 (brs, 3H), 7.77–7.75 (d, $J$ = 7.8 Hz, 1H), 7.64–7.60 (t, $J$ = 7.9 Hz, 1H), 7.08–7.04 (t, $J$ = 7.5 Hz, 1H), 3.83–3.80 (t, $J$ = 5.8 Hz, 2H), 3.03–2.99 (m, 4H), 2.66–2.60 (m, 2H). $^{13}$C NMR (100 MHz, DMSO-$d_6$): 167.6, 164.5, 147.9, 142.7, 136.8, 135.3, 129.9, 125.6, 123.1, 121.3, 36.8, 32.3, 32.2. Anal. ($C_{16}H_{16}F_3N_3O_6S$) Calcd. C: 44.14%, H: 3.70%, N: 9.65%; found C: 43.21%, H: 3.65%, N: 9.40%.

*5.6.7. 3-(2-Aminoethyl)-5-(3-(4-chlorophenyl)propylidene) thiazolidine-2,4-dione* ***8***

$^1$H NMR (400 MHz, DMSO-$d_6$): $\delta$ 7.89 (brs, 3H), 7.37–7.35 (d, $J$ = 7.8 Hz, 2H), 7.30–7.28 (d, $J$ = 7.8 Hz, 2H), 7.04–7.00 (t, $J$ = 7.5 Hz, 1H), 3.83–3.80 (t, $J$ = 5.9 Hz, 2H), 3.05–3.02 (t, $J$ = 5.9 Hz, 2H), 2.86–2.83 (t, $J$ = 5.9 Hz, 2H), 2.58–2.52 (m, 2H). $^{13}$C NMR (100 MHz, DMSO-$d_6$): 167.6, 164.5, 139.3, 137.1, 130.8, 130.2, 128.3, 125.4, 36.8, 32.5, 32.2. Anal. ($C_{16}H_{16}ClF_3N_2O_4S$) Calcd. C: 45.24%, H: 3.80%, N: 6.59%; found C: 45.06%, H: 3.66%, N: 6.61%.

*5.6.8. 3-(2-Aminoethyl)-5-(3-pyridin-3-yl-propylidene) thiazolidine-2,4-dione* ***11***

$^1$H NMR (400 MHz, DMSO-$d_6$): $\delta$ 8.90–8.89 (d, $J$ = 1.2 Hz, 1H), 8.79–8.77 (d, $J$ = 5.1 Hz, 1H), 8.50–8.48 (d, $J$ = 8.1 Hz, 1H), 8.21 (brs, 3H), 7.99–7.96 (dd, $J$ = 8.0, 5.6 Hz, 1H), 7.06 (t, $J$ = 7.5 Hz, 1H), 3.84 (t, $J$ = 6.0 Hz, 2H), 3.07 (t, $J$ = 7.3 Hz, 2H), 3.02–2.98 (m, 2H), 2.68–2.63 (q, $J$ = 7.4 Hz, 2H). $^{13}$C NMR (100 MHz, DMSO-$d_6$): 167.5, 164.4, 145.1, 141.9, 140.3, 140.0, 136.0, 126.6, 126.1, 38.9, 36.5, 31.6, 29.7. Anal. ($C_{13}H_{17}Cl_2N_3O_2S$) Calcd. C: 44.35%, H: 4.92%, N: 11.94%; found C: 44.35%, H: 4.85%, N: 11.90%.

*5.6.9. 3-(2-Aminoethyl)-5-(3-indol-3-yl-propylidene)thiazolidine-2,4-dione* ***12***

$^1$H NMR (400 MHz, $CDCl_3$): $\delta$ 8.03 (brs, 1H), 7.58–7.56 (d, $J$ = 7.8 Hz, 1H), 7.38–7.36 (d, $J$ = 8.1 Hz, 1H), 7.22–7.11 (m, 3H), 7.01–7.00 (d, $J$ = 2.1 Hz, 1H), 3.74 (t, $J$ = 6.3 Hz, 2H), 3.02 (t, $J$ = 7.3 Hz, 2H), 2.93 (t, $J$ = 6.3 Hz, 2H), 2.68–2.62 (q, $J$ = 7.4 Hz, 2H). $^{13}$C NMR (100 MHz, $CDCl_3$): 168.1, 165.3, 138.3, 136.4, 127.1, 125.6, 122.3, 121.6, 119.5, 118.6, 114.4, 111.3, 44.5, 40.0, 32.4, 23.6. Anal. ($C_{16}H_{18}ClN_3O_2S$) Calcd. C: 54.62%, H: 5.16%, N: 11.94%; found C: 54.59%, H: 5.18%, N: 11.90%.

*5.6.10. 3-(2-Aminoethyl)-5-(5-indol-3-yl-propylidene)thiazolidine-2,4-dione* ***13***

$^1$H NMR (400 MHz, $CDCl_3$): 8.15 (brs, 1H), 7.45 (s, 1H), 7.34–7.32 (d, $J$ = 8.3 Hz, 1H), 7.20 (t, $J$ = 2.9 Hz, 1H), 7.14 (t, $J$ = 7.6 Hz, 1H), 7.03–7.01 (dd, $J$ = 8.3 Hz, 1.6 Hz, 1H), 6.51–6.50 (m, 1H), 3.74 (t, $J$ = 6.3 Hz, 2H), 2.96–2.92 (m, 4H), 2.62–2.57 (q, $J$ = 7.6 Hz, 2H); $^{13}$C NMR (100 MHz, $CDCl_3$): 168.1, 165.3, 138.1, 134.7, 131.3, 128.2, 125.6, 124.6, 122.7, 120.0, 111.2, 102.4, 44.5, 40.0, 34.3, 34.1. Anal. ($C_{16}H_{18}ClN_3O_2S$) Calcd. C: 54.62%, H: 5.16%, N: 11.94%; found C: 54.70%, H: 5.10%, N: 11.87%.

*5.6.11. 3-(2-Aminoethyl)-5-propylidenethiazolidine-2,4-dione* ***14***

$^1$H NMR (400 MHz, DMSO-$d_6$): $\delta$ 8.27 (brs, 3H), 7.12–7.08 (t, $J$ = 7.6 Hz, 1H), 3.93–3.90 (t, $J$ = 6.0 Hz, 2H), 3.07 (m, 2H), 2.33–2.26 (m, 2H), 1.17–1.13 (t, $J$ = 7.5 Hz, 3H). $^{13}$C NMR (100 MHz, DMSO-$d_6$): 167.6, 164.7, 139.4, 124.3, 36.5, 24.6, 12.1. Anal. ($C_8H_{13}ClN_2O_2S$) Calcd. C: 40.59%, H: 5.54%, N: 11.83%; found C: 40.39%, H: 5.42%, N: 11.60%.

*5.6.12. 3-(2-Aminoethyl)-5-(3-cyclohexyl-propylidene) thiazolidine-2,4-dione* ***15***

$^1$H NMR (400 MHz, DMSO-$d_6$): $\delta$ 8.16 (brs, 3H), 7.05–7.01 (t, 1H), 3.87–3.84 (t, $J$ = 6.0 Hz, 2H), 3.03–3.00 (t, $J$ = 6.0 Hz, 2H), 2.26–2.21 (q, $J$ = 7.6 Hz, 2H), 1.70–1.60 (m, 5H), 1.42–1.37 (q, $J$ = 7.3 Hz, 2H), 1.27–1.10 (m, 4H), 0.92–0.83 (m, 2H). $^{13}$C NMR (100 MHz, DMSO-$d_6$): 167.6, 164.6, 138.5, 124.7, 36.5, 34.6, 34.7, 32.5, 28.6, 26.0, 25.6. Anal. ($C_{14}H_{23}ClN_2O_2S$) Calcd. C: 52.73%, H: 7.27%, N: 8.79%; found C: 52.87%, H: 7.17%, N: 8.79%.

*5.6.13. 3-(2-Aminoethyl)-5-(3-cyclopropyl-propylidene) thiazolidine-2,4-dione* ***16***

$^1$H NMR (400 MHz, DMSO-$d_6$): $\delta$ 8.13 (brs, 3H), 7.06 (t, $J$ = 7.7 Hz, 1H), 3.83 (t, $J$ = 6.0 Hz, 2H), 3.00 (m, 2H), 2.32–2.26 (q, $J$ = 7.4 Hz, 2H), 1.43–1.37 (q, $J$ = 7.1 Hz, 2H), 0.72–0.68 (m, 1H), 0.42–0.38 (m, 2H), 0.06–0.03 (m, 2H). $^{13}$C NMR (100 MHz, DMSO-$d_6$): 167.6, 164.6, 138.1, 124.9, 36.6, 32.2, 31.6, 10.4, 4.5. Anal. ($C_{11}H_{17}ClN_2O_2S$) Calcd. C: 47.73%, H: 6.19%, N: 10.12%; found C: 47.67%, H: 6.19%, N: 10.12%.

*5.6.14. 3-(2-Hydroxyethyl)-5-(3-phenyl-propylidene)thiazolidine-2,4-dione* ***17***

$^1$H NMR (400 MHz, $CDCl_3$): $\delta$ 7.33–7.31 (m, 2H), 7.24–7.18 (m, 3H), 7.11 (t, $J$ = 7.7 Hz, 1H), 3.91 (t, $J$ = 5.0 Hz, 2H), 3.84–3.83 (m, 2H), 2.86 (t, $J$ = 7.5 Hz, 2H), 2.59–2.53 (q, $J$ = 7.6 Hz, 2H). $^{13}$C NMR (100 MHz, $CDCl_3$): 168.2, 165.5, 139.8, 137.8, 128.7, 128.3, 126.6, 125.7, 60.4, 44.1, 33.9, 33.4. Anal. ($C_{14}H_{15}NO_3S\cdot 0.10H_2O$) Calcd. C: 60.24%, H: 5.49%, N: 5.02%; found C: 60.13%, H: 5.47%, N: 4.84%.

*5.6.15. [5-(3-Phenyl-propylidene)thiazolidine-2,4-dione-3-yl]-acetic acid* ***18***

$^1$H NMR (400 MHz, $CDCl_3$): $\delta$ 7.32–7.29 (m, 2H), 7.24–7.23 (m, 1H), 7.20–7.17 (m, 2H), 7.14 (t, $J$ = 7.7 Hz, 1H), 4.46 (s, 2H), 2.86 (t, $J$ = 7.5 Hz, 2H), 2.59–2.54 (q, $J$ = 7.6 Hz, 2H). $^{13}$C NMR (100 MHz, CDCl3): 171.5, 167.0, 164.0, 139.7, 138.6, 128.7, 128.3, 126.6, 125.4, 41.4, 33.8, 33.5. Anal. ($C_{14}H_{13}NO_4S$) Calcd. C: 57.72%, H: 4.50%, N: 4.81%; found C: 57.42%, H: 4.51%, N: 4.74%.

*5.6.16. 3-(2-Morpholin-ethyl)-5-(3-phenyl-propylidene) thiazolidine-2,4-dione* ***19***

$^1$H NMR (400 MHz, $CDCl_3$): $\delta$ 7.32–7.18 (m, 5H), 7.08–7.05 (t, $J$ = 7.6 Hz, 1H), 3.81–3.78 (t, $J$ = 6.4 Hz, 2H), 3.65–3.62 (t, $J$ = 4.6 Hz, 4H), 2.88–2.84 (t, $J$ = 7.5 Hz, 2H), 2.58–2.54 (m, 4H), 2.49–2.47 (t, $J$ = 4.5 Hz, 4H). $^{13}$C NMR (100 MHz, $CDCl_3$): 167.6, 164.9, 139.9, 136.9, 128.7, 128.3, 126.6, 126.0, 67.0, 55.2, 53.5, 38.6, 33.9, 33.4. Anal. ($C_{18}H_{22}N_2O_3S$) Calcd. C: 62.40%, H: 6.40%, N: 8.09%; found C: 62.39%, H: 6.53%, N: 7.90%.

*5.7. Preparation of 3-(2-aminoethyl)-5-(3-phenyl-propyl) thiazolidine-2,4-dione* ***20***

Compound **1** (55.2 mg, 0.2 mmol) and 10% Pd/C (50.0 mg) in MeOH (10.0 mL) was hydrogenated (60 psi) at room temperature for 15 h. The reaction was filtered through a short bed of celite and the filtrate was concentrated under reduced pressure to give **20** as white solid. $^1$H NMR (400 MHz, DMSO-$d_6$): $\delta$ 8.07(brs, 3H), 7.31–7.17 (m, 5H), 4.57–4.54 (dd, $J$ = 4.5, 8.9 Hz, 1H), 3.76–3.73 (t, $J$ = 6.1 Hz, 2H), 3.01–2.93 (m, 2H), 2.65–2.61 (m, 2H), 2.13–2.05 (m, 1H), 1.91–1.75 (m, 2H), 1.65–1.57 (m, 1H); $^{13}$C NMR (100 MHz, DMSO-$d_6$): 174.7, 171.6, 141.3, 128.3, 128.2, 125.8, 49.6, 36.5, 34.5, 31.2, 28.3. Anal. ($C_{14}H_{19}ClN_2O_2S$) Calcd. C: 53.41%, H: 6.08%, N: 8.90%; found C: 53.38%, H: 6.03%, N: 8.79%.

*5.7.1. N-(4-Iodo-phenyl)-methanesulfonamide* ***36***

To a stirred solution of 4-iodo-phenylamine **17** (1.1 g, 5.0 mmol) and $Et_3N$ (0.8 mL, 5.5 mmol) in DCM (20.0 mL) was added methanesulfonyl chloride (0.4 mL, 5.5 mmol) slowly. The reaction was stirred for 2 h, then water was added. The organic layer was extracted by 1 M NaOH and the aqueous phase was washed with DCM, and then was acidified with 1 M HCl to pH = 2–3. The aqueous phase was then extracted with DCM (2 × 20 mL) and dried over anhydrous $Na_2SO_4$. After filtration, the solvent was removed under educed pressure to give a white solid (492.0 mg). $^1$H NMR (400 MHz, $CDCl_3$): $\delta$ 7.68–7.66 (d, $J$ = 8.7 Hz, 2H), 6.99–6.97 (d, $J$ = 8.6 Hz, 2H), 3.01 (s, 3H).

*5.8. Procedure F. Preparation of N-(4-{3-[3-(2-aminoethyl)-2,4-dioxo-thiazolidin-5-ylidene]-propyl}-phenyl)-methanesulfonamide* ***9***

A mixture of **36** (178.0 mg, 0.6 mmol), allyl alcohol (0.06 mL, 0.9 mmol), $NaHCO_3$ (125.0 mg, 1.5 mmol), $Pd(OAc)_2$ (7.0 mg), TBACl (180.0 mg), and 4 Å sieves (100.0 mg) in DMF (2.0 mL) was stirred at room temperature for 48 h. The mixture was poured into water, extracted with diethyl ether, and dried over anhydrous $Na_2SO_4$. After removal of solvents, the residue was reacted with **31** following procedure E to give (2-{5-[3-(4-methanesulfonylamino-phenyl)-propylidene]-2,4-dioxo-thiazolidin-3-yl}-ethyl)-carbamic acid *tert*-butyl ester as an oil (70.0 mg). $^1$H NMR (400 MHz, $CDCl_3$): $\delta$ 7.20–7.15 (m, 4H), 7.05 (t, $J$ = 7.6 Hz, 1H), 6.83 (s, 1H), 4.79 (brs, 1H), 3.81 (t, $J$ = 5.9 Hz, 2H), 3.38–3.37 (m, 2H), 2.99 (s, 3H), 2.83 (t, $J$ = 7.5 Hz, 2H), 2.55–2.50 (q, $J$ = 7.6 Hz, 2H), 1.41 (s, 9H).

To the solution of (2-{5-[3-(4-methanesulfonylamino-phenyl)-propylidene]-2,4-dioxo-thiazolidin-3-yl}-ethyl)-carbamic acid *tert*-butyl ester (70.0 mg, 0.2 mmol) in ethyl acetate (3.0 mL) was added 4 M HCl in 1,4-dioxane (2.0 mL). The solution was stirred at room temperature for 5 h and filtered to give **9** as a light yellow solid. $^1$H NMR (400 MHz, DMSO-$d_6$): $\delta$ 9.66 (s, 1H), 8.03 (brs, 3H), 7.23–7.20 (d, $J$ = 8.5 Hz, 2H), 7.16–7.13 (d, $J$ = 8.5 Hz, 2H), 7.02 (t, $J$ = 7.5 Hz, 1H), 3.83 (t, $J$ = 5.9 Hz, 2H), 3.01–3.00 (m, 2H), 2.94 (s, 3H), 2.80 (t, $J$ = 7.3 Hz, 2H), 2.55–2.50 (q, $J$ = 7.3 Hz, 2H). $^{13}$C NMR (100 MHz, DMSO-$d_6$): 167.5, 164.4, 137.2, 136.4, 135.9, 129.0, 125.3, 120.2, 36.5, 32.6, 32.2. Anal. ($C_{15}H_{20}ClN_3O_4S_2$) Calcd. C: 44.38%, H: 4.97%, N: 10.35%; found C: 44.12%, H: 4.91%, N: 10.20%.

*5.8.1. 4-Iodo-benzenesulfonamide* ***39***

To the ammonium hydroxide (5.0 mL) was added 4-iodo-benzenesulfonyl chloride (454.0 mg, 1.5 mmol). The resulting mixture was stirred at room temperature for 2 h and extracted with DCM (2 × 20.0 mL). The combined organic phase was dried over anhydrous $Na_2SO_4$, and concentrated to give **39** as a white solid (392.0 mg). $^1$H NMR (400 MHz, DMSO-$d_6$): $\delta$ 7.98–7.96 (d, $J$ = 8.6 Hz, 2H), 7.60–7.58 (d, $J$ = 8.6 Hz, 2H), 7.45 (s, 2H).

*5.8.2. 4-{3-[3-(2-Aminoethyl)-2,4-dioxo-thiazolidin-5-ylidene]-propyl}-benzenesulfonamide **10***

Compound **39** (283.0 mg, 1.0 mmol) was reacted with allyl alcohol (0.1 mL, 1.5 mmol) followed by reaction with **31** following procedure F to give (2-{2,4-dioxo-5-[3-(4-sulfamoyl-phenyl)-propylidene]-thiazolidin-3-yl}-ethyl)-carbamic acid *tert*-butyl ester as an oil (80.0 mg). $^1$H NMR (400 MHz, $CDCl_3$): $\delta$ 7.88–7.86 (d, $J$ = 8.2 Hz, 2H) 7.34–7.32 (d, $J$ = 8.2 Hz, 2H), 7.02 (t, $J$ = 7.6 Hz, 1H), 4.75 (brs, 1H), 3.80 (t, $J$ = 5.9 Hz, 2H), 3.37–3.36 (m, 2H), 2.93 (t, $J$ = 7.5 Hz, 2H), 2.59–2.56 (q, $J$ = 7.6 Hz, 2H), 1.40 (s, 9H).

(2-{2,4-Dioxo-5-[3-(4-sulfamoyl-phenyl)-propylidene]-thiazolidin-3-yl}-ethyl)-carbamic acid *tert*-butyl ester (80.0 mg, 0.2 mmol) was treated with HCl in 1,4-dioxane following Procedure F to give **10** as a light yellow solid. $^1$H NMR (400 MHz, DMSO-$d_6$): $\delta$ 8.06 (brs, 3H), 7.76–7.74 (d, $J$ = 8.3 Hz, 2H), 7.47–7.44 (d, $J$ = 8.4 Hz, 2H), 7.30 (s, 2H), 7.02 (t, $J$ = 7.4 Hz, 1H), 3.83 (t, $J$ = 6.0 Hz, 2H), 3.03–2.98 (m, 2H), 2.93 (t, $J$ = 7.4 Hz, 2H), 2.61–2.56 (q, $J$ = 7.3 Hz, 2H); $^{13}$C NMR (100 MHz, DMSO-$d_6$): 167.4, 164.4, 144.4, 142.1, 136.8, 128.7, 125.7, 125.4, 36.5, 32.6, 32.1. Anal. ($C_{14}H_{18}ClN_3O_4S_2 \cdot 0.25H_2O$) Calcd. C: 42.42%, H: 4.70%, N: 10.60%; found C: 42.63%, H: 4.74%, N: 10.24%.

*5.8.3. 2-(2-(tert-Butoxycarbonylamino)ethyl)-1,3-dioxoisoindoline-5-carboxylic acid **42***

A mixture of *N-tert*-butoxycarbonyl-1,2-diaminoethane (2.0 g, 12.5 mmol), phthalic anhydride 41 (2.9 g, 15.0 mmol), and $Et_3N$ (2.2 mL, 10.0 mmol) in THF (120.0 mL) was refluxed for 3 h. The reaction mixture was concentrated, and the residue was purified by flash chromatography (DCM/MeOH = 9/1) to give **42** as a white crystal. $^1$H NMR (400 MHz, DMSO-$d_6$): $\delta$ 13.7 (brs, 1H), 8.36–8.34 (d, $J$ = 7.6 Hz, 1H), 8.21 (s, 1H), 7.99–7.97 (d, $J$ = 7.6 Hz, 1H), 6.95–6.92 (s, 1H), 3.66–3.63 (m, 2H), 3.20–3.18 (m, 2H), 1.26 (m, 9H). $^{13}$C NMR (100 MHz, DMSO-$d_6$): 167.1, 165.8, 155.7, 136.0, 135.2, 135.0, 132.3, 123.2, 122.7, 77.6, 38.2, 37.9, 28.0.

*5.8.4. tert-Butyl 2-(5-(hydroxymethyl)-1,3-dioxoisoindolin-2-yl) ethylcarbamate **43***

To a solution of **42** (588.0 mg, 1.8 mmol) in THF (10.0 mL) was added $BH_3 \cdot THF$ (1.0 M THF solution, 2.1 mL, 2.1 mmol) at 0 °C, and the mixture was stirred at room temperature overnight. The reaction was quenched by adding 2.0 mL of $H_2O$. The mixture was extracted with ethyl acetate (2 × 20.0 mL), washed with brine, dried over anhydrous $Na_2SO_4$, and evaporated under reduced pressure. The residue was purified by flash chromatography (hexane/EtOAc = 4/6) to give **43** as a white solid. $^1$H NMR (400 MHz, $CDCl_3$): $\delta$ 7.85–7.82 (d, $J$ = 7.7 Hz, 1H), 7.80 (s, 1H), 7.71–7.69 (d, $J$ = 7.7 Hz, 1H), 4.85 (s, 2H), 3.83–3.81 (t, $J$ = 5.6 Hz, 2H), 3.44–3.41 (m, 2H), 1.34 (m, 9H). $^{13}$C NMR (100 MHz, DMSO-$d_6$): 168.4, 156.0, 148.2, 132.5, 131.8, 131.0, 123.4, 121.3, 79.5, 64.2, 39.6, 38.1, 28.2.

*5.8.5. tert-Butyl 2-(5-((diethoxyphosphoryloxy)-methyl)-1,3-dioxoisoindolin-2-yl)-ethylcarbamate **44***

To a flask charged with **43** (0.2 g, 0.6 mmol), $Et_3N$ (0.1 mL, 1.0 mmol, 150 mol%), DMAP (7.6 mg, 0.06 mmol, 10 mol%) and THF (10.0 mL) was added diethyl chlorophosphate (0.1 mL, 0.8 mmol, 120 mol%) over 30 min at 0 °C. The resulting mixture was stirred for 16 h at room temperature, then quenched with EtOAc/$H_2O$ (1/1, 30.0 mL). The aqueous phase was extracted with EtOAc (2 × 20.0 mL) and the combined organic phase was then washed with saturated $NaHCO_3$ (30.0 mL) and brine (30.0 mL), and dried over anhydrous $Na_2SO_4$. After removal of solvents under reduced pressure, the crude oil was purified by flash chromatography (EtOAc/hexane = 6/4) to give **44** as white solid. $^1$H NMR (400 MHz, $CDCl_3$): $\delta$ 7.87–7.86 (d, $J$ = 7.7 Hz, 1H), 7.84 (s, 1H), 7.74–7.72 (d, $J$ = 7.7 Hz, 1H), 5.18 (s, 2H), 4.17–4.11 (m, 4H), 3.85–3.82 (t, $J$ = 5.6 Hz, 2H), 3.43–3.42 (m, 2H), 1.40–1.33 (m, 15H). $^{13}$C NMR (100 MHz, DMSO-$d_6$): 167.9, 132.7, 132.6, 131.9, 123.4, 121.9, 67.6, 65.1, 64.1, 38.2, 28.2, 16.1.

*5.8.6. 2-(2-Aminoethyl)-5-benzylisoindoline-1,3-dione **21***

$Pd(OAc)_2$ (1.1 mg, 1.0 mol%) and $Ph_3P$ (5.1 mg, 4.0 mol%) were dissolved in toluene (1.0 mL) and transferred into flask containing **44** (0.2 g, 1.0 mmol), benzeneboronic acid (64.7 mg, 1.1 mmol) and $K_3PO_4$ (0.1 g, 1.1 mmol). The vigorously stirred mixture was heated to 90 °C for 16 h under $N_2$. The mixture was quenched with $H_2O$ (10.0 mL) and extracted with EtOAc (2 × 20.0 mL). The combined organic phase was washed with brine and $H_2O$, then dried over anhydrous $Na_2SO_4$. After removal of solvents under reduced pressure, the residue was purified by flash chromatography (EtOAc/hexane = 3/7) to give Boc-protected **21**. $^1$H NMR (400 MHz, $CDCl_3$): $\delta$ 7.76–7.74 (d, $J$ = 7.6 Hz, 1H), 7.66 (s, 1H), 7.54–7.52 (d, $J$ = 7.5 Hz, 1H), 7.33–7.16 (m, 5H), 4.80 (brs, 1H), 4.10 (s, 2H), 3.80 (t, $J$ = 5.4 Hz, 2H), 3.41–3.40 (m, 2H), 1.77 (s, 9H). $^{13}$C NMR (100 MHz, $CDCl_3$): 139.2, 134.4, 132.6, 128.9, 128.8, 126.8, 123.8, 123.5, 42.2, 28.2.

Boc-protected **21** was dissolved in anhydrous EtOAc (4.0 mL), and was added HCl solution (1.0 mL, 4 M in 1,4-dioxane). The mixture was stirred for 2 h at room temperature and the precipitate was filtered and washed with anhydrous diethyl ether to obtain **21** as a white solid. $^1$H NMR (400 MHz, DMSO-$d_6$): $\delta$ 8.07 (brs, 3H), 7.82–7.80 (d, 1H), 7.75–7.73 (m, 2H), 7.33–7.29 (m, 5H), 4.15 (s, 2H), 3.84–3.81 (t, $J$ = 5.9 Hz, 2H), 3.06–3.03 (t, $J$ = 5.9 Hz, 2H). $^{13}$C NMR (100 MHz, DMSO-$d_6$): 167.9, 167.8, 148.8, 140.2, 134.4, 132.5, 129.8, 128.8, 126.4, 123.2, 123.1, 40.8, 37.3, 35.2. Anal. ($C_{17}H_{17}ClN_2O_2 \cdot 0.5H_2O$) Calcd. C: 62.67%, H: 5.57%, N: 8.60%; found C: 62.99%, H: 5.27%, N: 8.69%.

*5.9. Biological assays*

Human leukemia U937 cells and human prostate cancer DU145 and PC-3 cells were obtained from American Type Culture Collection (ATCC, Manassas, VA). Human prostate cancer M12 cells were gift from Dr. Joye Ware from the Department of Pathology, VCU. U937, PC-3, M12 and DU145 cells were cultured in RPMI 1640 medium (Life Technologies, Inc., Grand Island, NY) supplemented with 10% (v/v) of heat-inactivated fetal bovine serum (FBS, Hyclone, Logan, UT). All cells were maintained at 37 °C in a fully humidified atmosphere containing 5% $CO_2$. Cells were rendered quiescent by incubation for 16 h in FBS-free medium and were then growth stimulated with phorbol 12-myristate 13-acetate (PMA, 200.0 nM) for immunoblot assay. Alternatively, cells were treated with compounds for indicated time in growing media and cell culture lysates were analyzed by Western blot assay. The MEK inhibitor PD0184352 was purchased from Upstate Biotechnology (Lake Placid, NY). All reagents were prepared and used as recommended by their suppliers.

*5.9.1. Western blot assay*

Cells ($5 \times 10^5$/mL) were pretreated with compounds for 1 h and then were lysed by sonication in 1x sample buffer [62.5 mM Tris base (pH 6.8), 2% SDS, 50 mM DTT, 10% glycerol, 0.1% bromphenol blue, and 5 mg/mL each chymostatin, leupeptin, aprotinin, pepstatin, and soybean trypsin inhibitor] and boiled for 5 min. For analysis of phospho-proteins, 1 mM of sodium orthovanadate and sodium pyrophosphate was added to the sample buffer. Protein samples were collected from the supernatant after centrifugation of the samples at 12,800× $g$ for 5 min, and protein was quantified using Coomassie Protein Assay Reagent (Pierce, Rockford, IL). Equal amounts of protein (30.0 μg) were separated by SDS-PAGE on 4–10% tris/glycine gel (Bio-Rad) and electrotransferred onto a PVDF membrane (Bio-Rad). For blotting phospho-proteins, no SDS was

included in the transfer buffer. The blots were blocked with 5% milk in TBS-Tween 20 (0.1%) at room temperature for 1 h and probed with the appropriate dilution of primary antibody overnight at 4 °C. The blots were washed twice in TBS-Tween 20 for 15 min and then incubated with a 1:2000 dilution of horseradish peroxidase-conjugated secondary antibody (Kirkegaard & Perry, Gaithersburg, MD) in 5% milk/PBS-Tween 20 at room temperature for 1 h. After washing twice in TBS-Tween 20 for 15 min, the proteins were visualized by Western Blot Chemiluminescence Reagent (NEN Life Science Products, Boston, MA). Where indicated, the blots were re-probed with antibodies against α-tubulin (Calbiochem) to ensure equal loading and transfer of proteins. The following antibodies were used as primary antibodies: Cell Signaling, MA: phospho-p44/42 MAPK (Thr202/Tyr204) antibody (1:1000, rabbit polyclonal), p44/42 MAPK antibody (1:1000, rabbit polyclonal), phospho-MEK1/2 (1:1000, rabbit polyclonal), MEK1/2 (1:1000, rabbit polyclonal), phospho-Akt (Ser473) antibody (1:1000, rabbit polyclonal), phospho-AMPK (Thr172) antibody (1:1000, rabbit polyclonal), AMPKα (1:1000, rabbit polyclonal); phospho-4EBP1 (Ser65) (1:1000, rabbit polyclonal). Santa Cruz, CA: Akt1/2/3 (H-136) (1:1000, rabbit polyclonal).

*5.9.2. Cell proliferation assays*

Cells were seeded at a density of $2 \times 10^4$ cells (100 μL)/well in 96-well plates and treated with compounds for 24 h. Then, 20 μL of MTS (MTS, 3-(4,5-dimethylthiazol-2-yl)-5-(3-carboxymethoxy phenyl)-2-(4-sulfophenyl)-2*H*-tetrazolium), CellTiter 96 AQueous One Solution Cell Proliferation Assay (Promega, Madison, WI) was added to each well, and the cells were incubated for an additional 1 h at 37 °C in a fully humidified atmosphere containing 5% $CO_2$. The intracellular soluble formazan produced by cellular reduction of the MTS was determined by recording the absorbance of each 96-well plates using the FlexStation 3 plate reader (Molecular Devices, CA) at a wavelength of 490 nm. Values were expressed as a percentage relative to those obtained in untreated controls.

*5.9.3. [$^3$H]-Thymidine incorporation assay*

The U937 cells ($2 \times 10^4$/well) were cultured with the compounds at various concentrations for 1 h or 24 h in the presence of 1 μCi [$^3$H]-thymidine. The cells were collected with a Tomtec Harvester 96 Mach III (Hamden, CT) and counted in a Perkin Elmer Wallac Microbeta Trilux Liquid Scintillation counter (Model 1450, Waltham, MA). The incorporation of [$^3$H]-thymidine into the proliferating cells was assayed and the data were expressed as % inhibition.

*5.9.4. Apoptosis assay*

After treatment with compounds at indicated concentrations for indicated intervals, cells were washed twice with cold PBS and then suspended in 1x binding buffer (10 mM HEPES [*N*-2-hydroxyethylpiperazine-*N*′-2-ethanesulfonic acid]/NaOH, pH 7.4, 140 mM NaOH, 2.5 mM $CaCl_2$). The cells were incubated with annexin V–fluorescein isothiocyanate (FITC) (BD PharMingen, San Diego, CA) and 5 μg/mL propidium iodide (PI), and incubated for 15 min at room temperature in the dark per the manufacturer's instructions. The samples were analyzed by flow cytometry using a Becton Dickinson FACScan (Becton Dickinson, San Jose, CA) within 1 h to determine the percentage of cells displaying annexin V staining (early apoptosis) or both annexin V and PI staining (late apoptosis).

*5.9.5. Cell cycle analysis*

Cells ($1 \times 10^6$) were suspended and fixed in 67% ethanol/PBS overnight at 4 °C and were stained with 3.8 mM sodium citrate solution containing 10 μg/mL PI and 0.5 mg/mL RNase A (Sigma–Aldrich, St. Louis, MO) for 4 h at 4 °C in the dark. Cell cycle analysis was performed by flow cytometry using Verity Winlist software (Topsham, ME) to determine the percentage of cells in the $G_0/G_1$, S, $G_2$/M and sub-$G_1$ phases of the cell cycle.

*5.9.6. Statistical analysis*

Data are reported as mean ± SEM of at least three independent experiments. Statistical analysis was performed using one-way ANOVA with Holm-Sidak post hoc test. Differences were considered significant at $p < 0.05$. Analyses were performed using Origin 8 software on a Windows platform.

## Acknowledgments

We thank Dr. Joye Ware at Virginia Commonwealth University for kindly providing the MC12 cells. The work was supported in part by the PRIP award and new faculty start-up funds from Virginia Commonwealth University.

## References

[1] Cancer Facts and Figures. American Cancer Society, 2010.
[2] S. Schubbert, K. Shannon, G. Bollag, Hyperactive Ras in developmental disorders and cancer, Nat. Rev. Cancer 7 (2007) 295–308.
[3] S. Yoon, R. Seger, The extracellular signal-regulated kinase: multiple substrates regulate diverse cellular functions, Growth Factor. 24 (2006) 21–44.
[4] P.J. Roberts, C.J. Der, Targeting the Raf-MEK-ERK mitogen-activated protein kinase cascade for the treatment of cancer, Oncogene 26 (2007) 3291–3310.
[5] L.S. Steelman, S.L. Abrams, J. Whelan, F.E. Bertrand, D.E. Ludwig, J. Bäsecke, M. Libra, F. Stivala, M. Milella, A. Tafuri, P. Lunghi, A. Bonati, A.M. Martelli, J.A. McCubrey, Contributions of the Raf/MEK/ERK, PI3K/PTEN/Akt/mTOR and Jak/STAT pathways to leukemia, Leukemia 22 (2008) 686–707.
[6] B.T. Hennessy, D.L. Smith, P.T. Ram, Y. Lu, G.B. Mills, Exploiting the PI3K/AKT pathway for cancer drug discovery, Nat. Rev. Drug Discov. 4 (2005) 988–1004.
[7] R. Marone, V. Cmiljanovic, B. Giese, M.P. Wymann, Targeting phosphoinositide 3-kinase: moving towards therapy, Biochim. Biophys. Acta 1784 (2008) 159–185.
[8] L. Paz-Ares, C. Blanco-Aparicio, R. Garcia-Carbonero, A. Carnero, Inhibiting PI3K as a therapeutic strategy against cancer, Clin. Transl. Oncol. 11 (2009) 572–579.
[9] H. Gao, X. Ouyang, W.A. Banach-Petrosky, W.L. Gerald, M.M. Shen, C. Abate-Shen, Combinatorial activities of Akt and B-Raf/Erk signaling in a mouse model of androgen-independent prostate cancer, Proc. Natl. Acad. Sci. U. S. A. 103 (2006) 14477–14482.
[10] C.P. Paweletz, L. Charboneau, V.E. Bichsel, N.L. Simone, T. Chen, J.W. Gillespie, M.R. Emmert-Buck, M.J. Roth, E.F. Petricoin III, L.A. Liotta, Reverse phase protein microarrays which capture disease progression show activation of pro-survival pathways at the cancer invasion front, Oncogene 20 (2001) 1981–1989.
[11] M.M. Shen, C. Abate-Shen, Pten inactivation and the emergence of androgen-independent prostate cancer, Cancer Res. 67 (2007) 6535–6538.
[12] C.W. Kinkade, M. Castillo-Martin, A. Puzio-Kuter, J. Yan, T.H. Foster, H. Gao, Y. Sun, X. Ouyang, W.L. Gerald, C. Cordon-Cardo, C. Abate-Shen, Targeting AKT/mTOR and ERK MAPK signaling inhibits hormone-refractory prostate cancer in a preclinical mouse model, J. Clin. Invest. 118 (2008) 3051–3064.
[13] A. Carracedo, L. Ma, J. Teruya-Feldstein, F. Rojo, L. Salmena, A. Alimonti, A. Egia, A.T. Sasaki, G. Thomas, S.C. Kozma, A. Papa, C. Nardella, L.C. Cantley, J. Baselga, P.P. Pandolfi, Inhibition of mTORC1 leads to MAPK pathway activation through a PI3K dependent feedback loop in human cancer, J. Clin. Invest. 118 (2008) 3065–3074.
[14] S.L. Abrams, L.S. Steelman, J.G. Shelton, E.W. Wong, W.H. Chappell, J. Bäsecke, F. Stivala, M. Donia, F. Nicoletti, M. Libra, A.M. Martelli, J.A. McCubrey, The Raf/MEK/ERK pathway can govern drug resistance, apoptosis and sensitivity to targeted therapy, Cell Cycle 9 (2010) 1781–1791.
[15] Q.B. She, D.B. Solit, Q. Ye, K.E. O'Reilly, J. Lobo, N. Rosen, The BAD protein integrates survival signaling by EGFR/MAPK and PI3K/Akt kinase pathways in PTEN-deficient tumor cells, Cancer Cell 8 (2005) 287–297.
[16] P.J. Lambert, A.Z. Shahrier, A.G. Whitman, O.F. Dyson, A.J. Reber, J.A. McCubrey, S.M. Akula, Targeting the PI3K and MAPK pathways to treat Kaposi's-sarcoma-associated herpes virus infection and pathogenesis, Expert Opin. Ther. Targets 11 (2007) 589–599.
[17] M. Rahmani, A. Anderson, J.R. Habibi, T.R. Crabtree, M. Mayo, H. Harada, A. Ferreira-Gonzalez, P. Dent, S. Grant, The BH3-only protein Bim plays a critical role in leukemia cell death triggered by concomitant inhibition of the PI3K/Akt and MEK/ERK1/2 pathways, Blood 114 (2009) 4507–4516.
[18] S.L. Abrams, L.S. Steelman, J.G. Shelton, W. Chappell, J. Bäsecke, M. Donia, F. Nicoletti, M. Libra, A.M. Martelli, J.A. McCubrey, Enhancing therapeutic

efficacy by targeting non-oncogene addicted cells with combinations of signal transduction inhibitors and chemotherapy, Cell Cycle 9 (2010) 1839–1846.
[19] M.E. Welsch, S.A. Snyder, B.R. Stockwell, Privileged scaffolds for library design and drug discovery, Curr. Opin. Chem. Biol. 14 (2010) 347–361.
[20] Q. Zhang, H. Zhou, S. Zhai, B. Yan, Natural product-inspired synthesis of thiazolidine and thiazolidinone compounds and their anticancer activities, Curr. Pharm. Des. 16 (2010) 1826–1842.
[21] S.D. Knight, N.D. Adams, et al., Discovery of GSK2126458, a highly potent inhibitor of PI3K and the mammalian target of rapamycin, Med. Chem. Lett. 1 (2010) 39–43.
[22] W. Motomura, S. Tanno, N. Takahashi, M. Nagamine, M. Fukuda, Y. Kohgo, T. Okumura, Involvement of MEK-ERK signaling pathway in the inhibition of cell growth by troglitazone in human pancreatic cancer cells, Biochem. Biophys. Res. Commun. 332 (2005) 89–94.
[23] J.B. Baell, G.A. Holloway, New substructure filters for removal of pan assay interference compounds (PAINS) from screening libraries and for their exclusion in bioassays, J. Med. Chem. 53 (2010) 2719–2740.
[24] P.H. Carter, P.A. Scherle, et al., Photochemically enhanced binding of small molecules to the tumor necrosis factor receptor-1 inhibits the binding of TNF-α, Proc. Natl. Acad. Sci. U.S.A. 98 (2001) 11879–11884.
[25] Q. Li, A. Al-Ayoubi, T. Guo, H. Zheng, A. Sarkar, T. Nguyen, S.T. Eblen, S. Grant, G.E. Kellogg, S. Zhang, Structure–activity relationship (SAR) studies of 3-(2-amino-ethyl)-5-(4-ethoxy-benzylidene)thiazolidine-2,4-dione: development of potential substrate-specific ERK1/2 inhibitors, Bioorg. Med. Chem. Lett. 19 (2009) 6042–6046.
[26] Q. Li, J.D. Wu, H. Zheng, K. Liu, T. Guo, Y. Liu, S.T. Eblen, S. Grant, S. Zhang, Discovery of 3-(2-aminoethyl)-5-(3-phenyl-propylidene)-thiazolidine-2,4-dione as a dual inhibitor of the Raf/MEK/ERK and the PI3K/Akt signaling pathways, Bioorg. Med. Chem. Lett. 20 (2010) 4526–4530.
[27] C.G. Frost, B.C. Hartley, Tandem molybdenum catalyzed hydrosilylations: an expedient synthesis of β-aryl aldehydes, Org. Lett. 9 (2007) 4259–4261.
[28] Y. Momose, T. Maekawa, T. Yamano, M. Kawada, H. Odaka, H. Ikeda, T. Sohda, Novel 5-subsituted 2,4-thiazolidinedione and 2,4-oxazolidinedione derivatives as insulin sensitizers with antidiabetic activities, J. Med. Chem. 45 (2002) 1518–1534.
[29] M. McLaughlin, Suzuki–Miyaura cross-coupling of benzylic phosphates with arylboronic acids, Org. Lett. 7 (2005) 4875–4878.
[30] T. Hayashi, M.F. Hirshman, E.J. Kurth, W.W. Winder, L.J. Goodyear, Evidence for 5′AMP-activated protein kinase mediation of the effect of muscle contraction on glucose transport, Diabetes 47 (1998) 1369–1373.
[31] A.C. Racanelli, S.B. Rothbart, C.L. Heyer, R.G. Moran, Therapeutics by cytotoxic metabolite accumulation: pemetrxed causes ZMP accumulation, AMPK activation, and mammalian target of rapamycin inhibition, Cancer Res. 69 (2009) 5467–5474.
[32] O. Mace, A.M. Woollhead, D.L. Baines, AICAR activates AMPK and alters PIP2 association with the epithelial sodium channel ENaC to inhibit Na+ transport in H441 lung epithelial cells, J. Physiol. 586 (2008) 4541–4557.
[33] R.M. Memmott, P.A. Dennis, Akt dependent and independent mechanisms of mTOR regulation in cancer, Cell Signal. 21 (2009) 656–664.
[34] G. Jones, P. Willett, R.C. Glen, A.R. Leach, R. Taylor, Development and validation of a genetic algorithm for flexible docking, J. Mol. Biol. 267 (1997) 727–748.
[35] J.F. Ohren, H. Chen, A. Pavlovsky, C. Whitehead, E. Zhang, P. Kuffa, C. Yan, P. McConnell, C. Spessard, C. Banotai, W.T. Mueller, A. Delaney, C. Omer, J. Sebolt-Leopold, D.T. Dudley, I.K. Leung, C. Flamme, J. Warmus, M. Kaufman, S. Barrett, H. Tecle, C.A. Hasemann, Structures of human MAP kinase kinase 1 (MEK1) and MEK2 describe novel noncompetitive kinase inhibition, Nat. Struct. Mol. Biol. 11 (2004) 1192–1197.
[36] D. Mandelker, S.B. Gabelli, O. Schidt-Kittler, J. Zhu, I. Cheong, C.H. Huang, K.W. Kinzler, B. Vogelstein, L.M. Amzel, A frequent kinase domain mutation that changes the interaction between PI3K alpha and the membrane, Proc. Natl. Acad. Sci. U. S. A. 6 (2009) 16996–17001.
[37] G.E. Kellogg, D.J. Abraham, Hydrophobicity: is LogP(o/w) more than the sum of its parts? Eur. J. Med. Chem. 35 (2000) 651–661.
[38] S. Meloche, J. Pouyssegur, The ERK1/2 mitogen-activated protein kinase pathway as a master regulator of the G1- to S-phase transition, Oncogene 26 (2007) 3227–3239.
[39] F. Chang, J.T. Lee, P.M. Navolanic, L.S. Steelman, J.G. Shelton, W.L. Blalock, R.A. Franklin, J.A. McCubrey, Involvement of PI3K/Akt pathway in cell cycle progression, apoptosis, and neoplastic transformation: a target for cancer chemotherapy, Leukemia 17 (2003) 590–603.
[40] J.S. Sebolt-Leopold, D.T. Dudley, R. Herrera, K. Van Becelaere, A. Wiland, R.C. Gowan, H. Tecle, S.D. Barrett, A. Bridges, S. Przybranowski, W.R. Leopold, A.R. Saltiel, Blockade of the MAP kinase pathway suppresses growth of colon tumors in vivo, Nat. Med. 5 (1999) 810–816.